

The two-loop perturbative correction to the $(g - 2)_\mu$ HLbL at short distances

Johan Bijmens,^a Nils Hermansson-Truedsson,^b Laetitia Laub^b and Antonio Rodríguez-Sánchez^c

^a*Department of Astronomy and Theoretical Physics, Lund University, Sölvegatan 14A, SE 223-62 Lund, Sweden*

^b*Albert Einstein Center for Fundamental Physics, Institute for Theoretical Physics, Universität Bern, Sidlerstrasse 5, CH-3012 Bern, Switzerland*

^c*Université Paris-Saclay, CNRS/IN2P3, IJCLab, 91405 Orsay, France*

E-mail: johan.bijmens@thep.lu.se, nils@itp.unibe.ch, laub@itp.unibe.ch, arodriguez@ijclab.in2p3.fr

ABSTRACT: The short-distance behaviour of the hadronic light-by-light (HLbL) contribution to $(g - 2)_\mu$ has recently been studied by means of an operator product expansion in a background electromagnetic field. The leading term in this expansion has been shown to be given by the massless quark loop, and the non-perturbative corrections are numerically very suppressed. Here, we calculate the perturbative QCD correction to the massless quark loop. The correction is found to be fairly small compared to the quark loop as far as we study energy scales where the perturbative running for the QCD coupling is well-defined, i.e. for scales $\mu \gtrsim 1$ GeV. This should allow to reduce the large systematic uncertainty associated to high-multiplicity hadronic states.

KEYWORDS: Perturbative QCD, Precision QED

ARXIV EPRINT: [2101.09169](https://arxiv.org/abs/2101.09169)

Contents

1	Introduction	1
2	The HLbL tensor and a_μ^{HLbL}	3
3	The two-loop perturbative correction	7
4	Results for the $(g - 2)_\mu$ and phenomenological implications	12
5	Conclusions	14
A	Master integrals	15
B	Analytical formulae	17
B.1	Expansions	17
B.1.1	Side regions	18
B.1.2	Corner regions	20
B.2	Symmetric point	23

1 Introduction

The muon anomalous magnetic moment is one of the most precise measurements in particle physics. The world average [1] for the anomaly $a_\mu = (g - 2)/2$ is

$$a_\mu^{\text{exp}} = 116\,592\,089(54)(33) \times 10^{-11}. \quad (1.1)$$

The experimental accuracy is expected to improve with the now running experiment at Fermilab [2] and the planned experiment at J-PARC [3]. The Standard Model prediction [1] is

$$a_\mu^{\text{SM}} = 116\,591\,810(43) \times 10^{-11}. \quad (1.2)$$

The difference between this and the experimental value from Brookhaven National Laboratory [4] is

$$\Delta a_\mu \equiv a_\mu^{\text{exp}} - a_\mu^{\text{SM}} = 279(76) \times 10^{-11}, \quad (1.3)$$

or a 3.7σ discrepancy. In light of this discrepancy and the expected improved experimental accuracy it is important that the theoretical accuracy is checked as much as possible. The QED [5, 6] and the electroweak contribution [7, 8] are precise enough for the foreseeable future. The error is dominated by the hadronic contributions, the hadronic vacuum polarization [9–15] is at present the largest theory uncertainty but is steadily being improved. The remaining part, the hadronic light-by-light (HLbL) contribution is at present [1]

$$a_\mu^{\text{HLbL}} = 92(18) \times 10^{-11}. \quad (1.4)$$

This number contains the next-to-leading (NLO) HLbL contribution [16] and the average of the lattice [17] and phenomenological evaluation of the lowest-order HLbL. In the remainder we will use HLbL as a synonym for the LO part only, this contribution is depicted in figure 1. The number in (1.4) is in good agreement with the older estimates [18–22] and the more recent Glasgow consensus [23] but with a smaller and much better understood error.

The phenomenological estimate of the HLbL [1],

$$a_{\mu}^{\text{HLbL-phen}} = 92(19) \times 10^{-11}, \tag{1.5}$$

uses the methods of ref. [24] to separate different contributions. The pole contributions from π^0, η, η' [25–27] as well as the two-pion box and rescattering and two-kaon box contribution [28] are well-understood and together give

$$a_{\mu}^{\text{HLbL-1}} = 69.4(4.1) \times 10^{-11}. \tag{1.6}$$

The main uncertainty comes from the intermediate and short-distance domain. Heavier intermediate states have been considered in refs. [29–34]. The heavy-quark contribution from charm is sufficiently well estimated from the quark loop and estimates of non-perturbative contributions and that of the bottom and top quarks are negligible [1, 35–37]. The light-quark contribution can be estimated using the quark loop and/or higher resonance exchanges and leads to [1]

$$a_{\mu}^{\text{HLbL-SD1}} = 20(19) \times 10^{-11}. \tag{1.7}$$

The large error is due to the large uncertainty of which resonances to include and that their couplings to two off-shell photons are badly known [1]. In addition one needs to make sure that there is a proper matching with the short-distance QCD constraints.

Some short-distance constraints are used in determining the form-factors needed in the contributions from hadrons directly, see e.g. ref. [38]. Here we discuss instead the short-distance constraints on the hadronic function defined in (2.1) and depicted as the shaded blob in figure 1. First attempts at matching the short-distance were using the quark loop and matching it on a long-distance contribution from the extended Nambu-Jona-Lasinio model [19]. The quark loop itself has a long history of being used in this context, see e.g. refs. [39–44]. The first proper short-distance constraint was derived in ref. [45]. It is valid in the regime where two of the internal photons have a virtuality much larger than the third one. Recent work in the latter regime includes refs. [36, 37, 46–52].

This paper is concerned with the limit where all virtualities of the internal photon lines in figure 1 are large. The underlying problem here is that the external photon, corresponding to the magnetic field, has zero momentum, i.e. $q_4 \rightarrow 0$ in figure 1. The usual operator product expansion (OPE) in vacuum [53] corresponds to all four photon virtualities large and diverges when setting $q_4 \rightarrow 0$. The solution was found in ref. [54]. One needs to use an alternative OPE in a background magnetic field as was done for the QCD sum rule calculations of nucleon magnetic moments [55, 56]. This method was earlier used in the context of the electroweak contribution to a_{μ} [7]. The first order term in this expansion corresponds to the massless quark loop [54], the next order is suppressed by

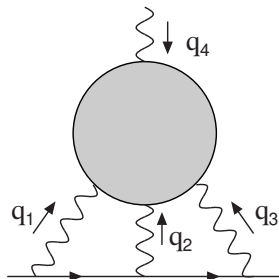


Figure 1. The HLbL contribution to the $(g - 2)_\mu$.

quark masses and the small value of the magnetic susceptibility [54, 57]. For the non-perturbative part of this OPE the contribution suppressed by up to four powers of large momenta compared to the leading term have been evaluated in ref. [57]. There are a number of subtleties involved and large number of expectation values in a magnetic field needed to be evaluated. The conclusion from [54, 57] is that the contribution from these higher orders in the non-perturbative part are small. The remaining uncertainty from this regime is the perturbative correction from gluon exchange to the massless quark loop. This paper performs that calculation. The putting together of this work with the other short-distance constraint [45] and the parts calculated using hadronic methods is deferred to future work.

In section 2 we recall the main definitions needed for the calculation of the HLbL part of a_μ . We define here a set of intermediate quantities, the $\tilde{\Pi}_i$ that are both ultraviolet and infrared finite. From these we then determine the quantities $\hat{\Pi}_i$ that are needed to calculate a_μ . The main procedure of the calculation is described in section 3. Section 4 gives the numerical results and discusses implications. We reiterate our main results in section 5. A number of technical issues are relegated to the appendices. The final result is too large to include in the manuscript but is included in the supplementary material.

2 The HLbL tensor and a_μ^{HLbL}

The HLbL tensor $\Pi^{\mu_1\mu_2\mu_3\mu_4}$ is a 4-point correlation function of electromagnetic currents $J^\mu(x) = \bar{q}(x) Q_q \gamma^\mu q(x)$, where the quark fields are collected in $q = (u, d, s)$ and the corresponding charge matrix is $Q_q = \text{diag}(e_q) = \text{diag}(2/3, -1/3, -1/3)$. The correlator in question is defined via

$$\Pi^{\mu_1\mu_2\mu_3\mu_4} = -i \int \frac{d^4 q_4}{(2\pi)^4} \left(\prod_{i=1}^3 \int d^4 x_i e^{-iq_i x_i} \right) \langle 0 | T \left(\prod_{j=1}^4 J^{\mu_j}(x_j) \right) | 0 \rangle, \quad (2.1)$$

where the q_i are the momenta of the external photon legs. This definition is slightly unconventional but allows to exploit more of the symmetries, as remarked in ref. [57]. The contribution from the HLbL tensor to the $(g - 2)_\mu$ is depicted in figure 1. It involves a loop integration over q_1, q_2 and q_3 , whereas the fourth leg is in the static limit, i.e. $q_4 \rightarrow 0$.

The HLbL tensor satisfies the Ward identities $q_{i,\mu_i} \Pi^{\mu_1\mu_2\mu_3\mu_4} = 0$ for $i = 1, 2, 3, 4$, which implies [58]

$$\Pi^{\mu_1\mu_2\mu_3\mu_4} = -q_{4,\nu_4} \frac{\partial \Pi^{\mu_1\mu_2\mu_3\nu_4}}{\partial q_{4,\mu_4}}. \quad (2.2)$$

The whole information about the HLbL is then contained in its derivative. In fact, in the $(g-2)_\mu$ kinematics,

$$\lim_{q_4 \rightarrow 0} \frac{\partial \Pi^{\mu_1\mu_2\mu_3\nu_4}}{\partial q_4^{\mu_4}}, \quad (2.3)$$

there are only 19 independent Lorentz structures, which can be found by applying 19 independent projectors $P_{\mu_1\mu_2\mu_3\mu_4\nu_4}^{\tilde{\Pi}_i}$, this according to

$$\tilde{\Pi}_i = P_{\mu_1\mu_2\mu_3\mu_4\nu_4}^{\tilde{\Pi}_i} \lim_{q_4 \rightarrow 0} \frac{\partial \Pi^{\mu_1\mu_2\mu_3\nu_4}}{\partial q_4^{\mu_4}}. \quad (2.4)$$

A possible set of projectors is

$$P_{\mu_1\mu_2\mu_3\mu_4\nu_4}^{\tilde{\Pi}_1} = g_{\mu_1\mu_2} g_{\mu_3\nu_4} q_{1,\mu_4}, \quad (2.5)$$

$$P_{\mu_1\mu_2\mu_3\mu_4\nu_4}^{\tilde{\Pi}_2} = g_{\mu_2\mu_3} g_{\mu_1\nu_4} q_{2,\mu_4}, \quad (2.6)$$

$$P_{\mu_1\mu_2\mu_3\mu_4\nu_4}^{\tilde{\Pi}_3} = g_{\mu_3\mu_1} g_{\mu_2\nu_4} q_{3,\mu_4}, \quad (2.7)$$

$$P_{\mu_1\mu_2\mu_3\mu_4\nu_4}^{\tilde{\Pi}_4} = g_{\mu_2\mu_1} g_{\mu_3\nu_4} q_{2,\mu_4}, \quad (2.8)$$

$$P_{\mu_1\mu_2\mu_3\mu_4\nu_4}^{\tilde{\Pi}_5} = g_{\mu_3\mu_2} g_{\mu_1\nu_4} q_{3,\mu_4}, \quad (2.9)$$

$$P_{\mu_1\mu_2\mu_3\mu_4\nu_4}^{\tilde{\Pi}_6} = g_{\mu_1\mu_3} g_{\mu_2\nu_4} q_{1,\mu_4}, \quad (2.10)$$

$$P_{\mu_1\mu_2\mu_3\mu_4\nu_4}^{\tilde{\Pi}_7} = g_{\mu_1\nu_4} g_{\mu_2\mu_4} q_{2,\mu_3}, \quad (2.11)$$

$$P_{\mu_1\mu_2\mu_3\mu_4\nu_4}^{\tilde{\Pi}_8} = g_{\mu_2\nu_4} g_{\mu_3\mu_4} q_{3,\mu_1}, \quad (2.12)$$

$$P_{\mu_1\mu_2\mu_3\mu_4\nu_4}^{\tilde{\Pi}_9} = g_{\mu_3\nu_4} g_{\mu_1\mu_4} q_{1,\mu_2}, \quad (2.13)$$

$$P_{\mu_1\mu_2\mu_3\mu_4\nu_4}^{\tilde{\Pi}_{10}} = g_{\mu_1\mu_2} q_{1,\mu_3} q_{1,\nu_4} q_{2,\mu_4}, \quad (2.14)$$

$$P_{\mu_1\mu_2\mu_3\mu_4\nu_4}^{\tilde{\Pi}_{11}} = g_{\mu_2\mu_3} q_{2,\mu_1} q_{2,\nu_4} q_{3,\mu_4}, \quad (2.15)$$

$$P_{\mu_1\mu_2\mu_3\mu_4\nu_4}^{\tilde{\Pi}_{12}} = g_{\mu_3\mu_1} q_{3,\mu_2} q_{3,\nu_4} q_{1,\mu_4}, \quad (2.16)$$

$$P_{\mu_1\mu_2\mu_3\mu_4\nu_4}^{\tilde{\Pi}_{13}} = g_{\mu_1\nu_4} q_{1,\mu_2} q_{2,\mu_3} q_{3,\mu_4}, \quad (2.17)$$

$$P_{\mu_1\mu_2\mu_3\mu_4\nu_4}^{\tilde{\Pi}_{14}} = g_{\mu_2\nu_4} q_{2,\mu_3} q_{3,\mu_1} q_{1,\mu_4}, \quad (2.18)$$

$$P_{\mu_1\mu_2\mu_3\mu_4\nu_4}^{\tilde{\Pi}_{15}} = g_{\mu_3\nu_4} q_{3,\mu_1} q_{1,\mu_2} q_{2,\mu_4}, \quad (2.19)$$

$$P_{\mu_1\mu_2\mu_3\mu_4\nu_4}^{\tilde{\Pi}_{16}} = g_{\mu_2\nu_4} q_{2,\mu_1} q_{1,\mu_3} q_{3,\mu_4}, \quad (2.20)$$

$$P_{\mu_1\mu_2\mu_3\mu_4\nu_4}^{\tilde{\Pi}_{17}} = g_{\mu_3\nu_4} q_{3,\mu_2} q_{2,\mu_1} q_{1,\mu_4}, \quad (2.21)$$

$$P_{\mu_1\mu_2\mu_3\mu_4\nu_4}^{\tilde{\Pi}_{18}} = g_{\mu_1\nu_4} q_{1,\mu_3} q_{3,\mu_2} q_{2,\mu_4}, \quad (2.22)$$

$$P_{\mu_1\mu_2\mu_3\mu_4\nu_4}^{\tilde{\Pi}_{19}} = q_{3,\mu_1} q_{1,\mu_2} q_{2,\mu_3} q_{1,\nu_4} q_{2,\mu_4}, \quad (2.23)$$

which has been built in such a way that, combined with the crossing symmetries of the HLbL tensor, the $\tilde{\Pi}$ satisfy the following crossing symmetries

$$\begin{aligned}
 \tilde{\Pi}_1 &= C_{12}[\tilde{\Pi}_4], & \tilde{\Pi}_2 &= C_{12}[\tilde{\Pi}_6], & \tilde{\Pi}_3 &= C_{12}[\tilde{\Pi}_5], & \tilde{\Pi}_7 &= C_{12}[\tilde{\Pi}_7], & \tilde{\Pi}_8 &= C_{12}[\tilde{\Pi}_9], & \tilde{\Pi}_{10} &= C_{12}[\tilde{\Pi}_{10}], \\
 \tilde{\Pi}_{11} &= C_{12}[\tilde{\Pi}_{12}], & \tilde{\Pi}_{13} &= C_{12}[\tilde{\Pi}_{16}], & \tilde{\Pi}_{14} &= C_{12}[\tilde{\Pi}_{18}], & \tilde{\Pi}_{15} &= C_{12}[\tilde{\Pi}_{17}], & \tilde{\Pi}_{19} &= C_{12}[\tilde{\Pi}_{19}], \\
 \tilde{\Pi}_1 &= C_{13}[\tilde{\Pi}_5], & \tilde{\Pi}_2 &= C_{13}[\tilde{\Pi}_4], & \tilde{\Pi}_3 &= C_{13}[\tilde{\Pi}_6], & \tilde{\Pi}_7 &= C_{13}[\tilde{\Pi}_8], & \tilde{\Pi}_9 &= C_{13}[\tilde{\Pi}_9], & \tilde{\Pi}_{10} &= C_{13}[\tilde{\Pi}_{11}], \\
 \tilde{\Pi}_{12} &= C_{13}[\tilde{\Pi}_{12}], & \tilde{\Pi}_{13} &= C_{13}[\tilde{\Pi}_{17}], & \tilde{\Pi}_{14} &= C_{13}[\tilde{\Pi}_{16}], & \tilde{\Pi}_{15} &= C_{13}[\tilde{\Pi}_{18}], & \tilde{\Pi}_{19} &= C_{13}[\tilde{\Pi}_{19}].
 \end{aligned} \tag{2.24}$$

The operator C_{ij} interchanges two momenta q_i and q_j . Notice how, from the knowledge of five of them, for example $\tilde{\Pi}_{1,7,10,13,19}$, one can easily infer the rest from these crossing symmetries. These $\tilde{\Pi}_i$ are well-defined and are both ultraviolet and infrared finite to the order in α we are working. For our calculation we use two different sets of $\tilde{\Pi}_i$, related by gauge invariance, which thus provides a cross-check of our results.

An OPE is only valid for large Euclidean momenta [53]. As a consequence, it cannot be directly applied to the tensor in (2.1) for the $(g-2)_\mu$ kinematics, since by definition the external photon is soft, $q_4 \rightarrow 0$, even though the other Euclidean momenta are large, $-q_i^2 \equiv Q_i^2 \gg \Lambda_{\text{QCD}}^2$ [54, 57]. However, precisely the same fact allows one to connect the tensor in (2.1) to the OPE of the tensor operator with the background photon field

$$\Pi^{\mu_1\mu_2\mu_3}(q_1, q_2) = -\frac{1}{e} \int \frac{d^4 q_3}{(2\pi)^4} \left(\prod_{i=1}^3 \int d^4 x_i e^{-iq_i x_i} \right) \langle 0 | T \left(\prod_{j=1}^3 J^{\mu_j}(x_j) \right) | \gamma(q_4) \rangle. \tag{2.25}$$

The OPE in question holds for large photon virtualities $Q_1^2 \sim Q_2^2 \sim Q_3^2 \gg \Lambda_{\text{QCD}}^2$. In this expansion, any local operator with the same quantum numbers as $F_{\mu\nu}$, including $F_{\mu\nu}$ itself, can absorb the remaining soft static photon and, as a consequence, give a contribution [7, 54, 57]. Higher-dimensional operators are suppressed by extra powers of $\left(\frac{\Lambda_{\text{QCD}}}{Q_i}\right)^d$, providing a hierarchy of contributions with a systematic counting. A very detailed study of this OPE can be found in ref. [57], where the different power corrections were computed and found to be small compared to the leading contribution.¹ The leading term comes from the $F_{\mu\nu}$ operator itself and is given by the massless quark loop at order α_s^0 , and the leading mass effects are very small. In fact, this quark loop corresponds to the zero momentum limit of the derivative of the naive massless perturbative QCD tensor of (2.1), i.e.

$$\lim_{q_4 \rightarrow 0} \frac{\partial \Pi_{\text{pert}}^{\mu_1\mu_2\mu_3\nu_4}}{\partial q_4^{\mu_4}}. \tag{2.26}$$

In this work, we compute the leading α_s correction to the direct $F_{\mu\nu}$ contribution in the OPE of (2.25). This corresponds to a two-loop massless QCD calculation with three external legs off-shell.

Before discussing the gluonic correction to the quark loop in the next section, we first write down the quark loop result for the $\tilde{\Pi}_i$ basis. As will be remarked upon below, this basis

¹Obviously, the results of this expansion cannot be applied to the whole integral domain of (2.34), but it can be used, apart from matching resonance models, for directly evaluating the significant contributions coming from the regions where the OPE is valid.

was not used in ref. [57]. The whole solution for the quark loop can be simply written as

$$\begin{aligned} \frac{\pi^2 \tilde{\Pi}_1}{N_c e_q^4} &= C_{123}(0) \left(Q_3^2 - Q_1^2 \right) - 1 + Q_2^{-2} Q_3^2 + 2 Q_2^2 Q_3^{-2} - Q_1^2 Q_2^{-2} - 2 Q_1^2 Q_3^{-2} \\ &\quad + \log \frac{Q_2^2}{Q_3^2} \left(1 - Q_2^2 Q_3^{-2} - Q_1^2 Q_3^{-2} \right) \\ &\quad + \log \frac{Q_1^2}{Q_3^2} \left(-\frac{5}{2} + \frac{1}{2} Q_2^{-2} Q_3^2 + Q_2^2 Q_3^{-2} + \frac{1}{2} Q_1^2 Q_2^{-2} + Q_1^2 Q_3^{-2} \right), \end{aligned} \quad (2.27)$$

$$\begin{aligned} \frac{\pi^2 \tilde{\Pi}_7}{N_c e_q^4} &= C_{123}(0) \left(Q_3^2 - Q_2^2 - Q_1^2 \right) \\ &\quad + \log \frac{Q_2^2}{Q_3^2} \left(-1 - Q_2^2 Q_3^{-2} + Q_1^2 Q_3^{-2} \right) + \log \frac{Q_1^2}{Q_3^2} \left(-1 + Q_2^2 Q_3^{-2} - Q_1^2 Q_3^{-2} \right), \end{aligned} \quad (2.28)$$

$$\begin{aligned} \frac{\pi^2 \tilde{\Pi}_{10}}{N_c e_q^4} &= C_{123}(0) \left(\frac{1}{2} Q_3^4 - \frac{1}{2} Q_2^2 Q_3^2 - \frac{1}{2} Q_1^2 Q_3^2 + Q_1^2 Q_2^2 \right) \\ &\quad - \frac{1}{2} Q_3^2 + Q_2^2 - \frac{1}{2} Q_2^4 Q_3^{-2} + Q_1^2 + Q_1^2 Q_2^2 Q_3^{-2} - \frac{1}{2} Q_1^4 Q_3^{-2} \\ &\quad + \log \frac{Q_2^2}{Q_3^2} \left(-\frac{3}{4} Q_3^2 - \frac{1}{2} Q_2^2 + \frac{1}{4} Q_2^4 Q_3^{-2} + Q_1^2 - \frac{1}{4} Q_1^4 Q_3^{-2} \right) \\ &\quad + \log \frac{Q_1^2}{Q_3^2} \left(-\frac{3}{4} Q_3^2 + Q_2^2 - \frac{1}{4} Q_2^4 Q_3^{-2} - \frac{1}{2} Q_1^2 + \frac{1}{4} Q_1^4 Q_3^{-2} \right), \end{aligned} \quad (2.29)$$

$$\begin{aligned} \frac{\pi^2 \tilde{\Pi}_{13}}{N_c e_q^4} &= C_{123}(0) \left(\frac{1}{2} Q_3^4 - \frac{1}{2} Q_2^4 - Q_1^2 Q_3^2 + \frac{1}{2} Q_1^2 Q_2^2 \right) \\ &\quad + \frac{1}{4} Q_2^{-2} Q_3^4 - \frac{1}{2} Q_3^2 + \frac{1}{4} Q_2^2 - \frac{1}{2} Q_1^2 Q_2^{-2} Q_3^2 - \frac{1}{2} Q_1^2 + \frac{1}{4} Q_1^4 Q_2^{-2} \\ &\quad + \log \frac{Q_2^2}{Q_3^2} \left(-\frac{1}{4} Q_3^2 - \frac{7}{4} Q_2^2 + \frac{3}{4} Q_1^2 \right) \\ &\quad + \log \frac{Q_1^2}{Q_3^2} \left(-Q_3^2 + Q_2^2 + \frac{1}{4} Q_1^2 Q_2^{-2} Q_3^2 + \frac{1}{4} Q_1^2 - \frac{1}{4} Q_1^4 Q_2^{-2} \right), \end{aligned} \quad (2.30)$$

$$\begin{aligned} \frac{\pi^2 \tilde{\Pi}_{19}}{N_c e_q^4} &= C_{123}(0) \left(-\frac{1}{4} Q_3^6 + \frac{1}{4} Q_2^2 Q_3^4 + \frac{1}{4} Q_2^4 Q_3^2 - \frac{1}{4} Q_2^6 + \frac{1}{4} Q_1^2 Q_3^4 - \frac{3}{2} Q_1^2 Q_2^2 Q_3^2 + \frac{1}{4} Q_1^2 Q_2^4 \right. \\ &\quad \left. + \frac{1}{4} Q_1^4 Q_3^2 + \frac{1}{4} Q_1^4 Q_2^2 - \frac{1}{4} Q_1^6 \right) \\ &\quad + \frac{1}{2} Q_3^4 - Q_2^2 Q_3^2 + \frac{1}{2} Q_2^4 - Q_1^2 Q_3^2 - Q_1^2 Q_2^2 + \frac{1}{2} Q_1^4 \\ &\quad + \log \frac{Q_2^2}{Q_3^2} \left(\frac{1}{2} Q_3^4 + \frac{1}{2} Q_2^2 Q_3^2 - Q_2^4 - Q_1^2 Q_3^2 + \frac{1}{2} Q_1^2 Q_2^2 + \frac{1}{2} Q_1^4 \right) \\ &\quad + \log \frac{Q_1^2}{Q_3^2} \left(\frac{1}{2} Q_3^4 - Q_2^2 Q_3^2 + \frac{1}{2} Q_2^4 + \frac{1}{2} Q_1^2 Q_3^2 + \frac{1}{2} Q_1^2 Q_2^2 - Q_1^4 \right). \end{aligned} \quad (2.31)$$

Here N_c is the number of colours and $C_{123}(0)$ is a loop integral function that is defined in appendix A.

For the $(g-2)_\mu$ integration, it is convenient using the generic results of refs. [24, 28, 57]. Following them, the HLbL tensor can be expanded in a basis of 54 scalar functions Π_i

weighted with Lorentz structures $T_i^{\mu_1\mu_2\mu_3\mu_4}$,

$$\Pi^{\mu_1\mu_2\mu_3\mu_4} = \sum_{i=1}^{54} T_i^{\mu_1\mu_2\mu_3\mu_4} \Pi_i. \quad (2.32)$$

Using

$$\lim_{q_4 \rightarrow 0} \frac{\partial \Pi^{\mu_1\mu_2\mu_3\nu_4}}{\partial q_4^{\mu_4}} = \lim_{q_4 \rightarrow 0} \sum_{i=1}^{54} \frac{\partial T_i^{\mu_1\mu_2\mu_3\nu_4}}{\partial q_4^{\mu_4}} \Pi_i, \quad (2.33)$$

the 19 $\tilde{\Pi}_i$ defined in (2.4) can be identified with the static $q_4 \rightarrow 0$ limit of certain linear combinations of the Π_i . Denoting these linear combinations $\hat{\Pi}_i$ it can further be shown that for a_μ^{HLbL} only six $\hat{\Pi}_i$ contribute, namely $\hat{\Pi}_{1,4,7,17,39,54}$.² In particular, the a_μ^{HLbL} may be written [24, 28]

$$a_\mu^{\text{HLbL}} = \frac{2\alpha^3}{3\pi^2} \int_0^\infty dQ_1 \int_0^\infty dQ_2 \int_{-1}^1 d\tau \sqrt{1-\tau^2} Q_1^3 Q_2^3 \sum_{i=1}^{12} T_i(Q_1, Q_2, \tau) \bar{\Pi}_i(Q_1, Q_2, \tau). \quad (2.34)$$

The integration variable τ is defined via $Q_3^2 = Q_1^2 + Q_2^2 + 2\tau Q_1 Q_2$, the $T_i(Q_1, Q_2, \tau)$ are functions and the $\bar{\Pi}_i$ are functions of the six $\hat{\Pi}_i$. The latter set of functions is related to the $\hat{\Pi}_i$ through

$$\begin{aligned} \bar{\Pi}_1 &= \hat{\Pi}_1, & \bar{\Pi}_2 &= C_{23} [\hat{\Pi}_1], & \bar{\Pi}_3 &= \hat{\Pi}_4, & \bar{\Pi}_4 &= C_{23} [\hat{\Pi}_4], \\ \bar{\Pi}_5 &= \hat{\Pi}_7, & \bar{\Pi}_6 &= C_{12} [C_{13} [\hat{\Pi}_7]], & \bar{\Pi}_7 &= C_{23} [\hat{\Pi}_7], \\ \bar{\Pi}_8 &= C_{13} [\hat{\Pi}_{17}], & \bar{\Pi}_9 &= \hat{\Pi}_{17}, & \bar{\Pi}_{10} &= \hat{\Pi}_{39}, \\ \bar{\Pi}_{11} &= -C_{23} [\hat{\Pi}_{54}], & \bar{\Pi}_{12} &= \hat{\Pi}_{54}. \end{aligned} \quad (2.35)$$

In summary, knowledge of $\hat{\Pi}_{1,4,7,17,39,54}$ is enough to determine a_μ^{HLbL} from (2.34). The $\hat{\Pi}_i$ can be obtained from the derivative of the HLbL tensor in the static limit with the projectors given in ref. [57]. There we defined

$$\hat{\Pi}_i = P_{\hat{\Pi}_i \mu_1 \mu_2 \mu_3 \mu_4 \nu_4} \lim_{q_4 \rightarrow 0} \frac{\partial \Pi^{\mu_1 \mu_2 \mu_3 \nu_4}}{\partial q_{4, \mu_4}}. \quad (2.36)$$

with the projectors $P_{\hat{\Pi}_i \mu_1 \mu_2 \mu_3 \mu_4 \nu_4}$ given in appendix A of [57]. Using the definitions of the $\tilde{\Pi}$ in (2.4) the relation between the $\hat{\Pi}$ and the $\tilde{\Pi}$ follows immediately. We have checked that this procedure reproduces the massless quark loop results as given in ref. [57]. The $\tilde{\Pi}_i$ representation of the massless quark loop was given in (2.27)–(2.31), and it can be noted that it is much simpler than the expressions for the $\hat{\Pi}_i$ in ref. [57].

3 The two-loop perturbative correction

In this section we present the calculation of the two-loop contribution. For the analytic calculation we use FORM [59]. The master integral reduction is done by means of Kira [60],

²Using the set of projectors defined in ref. [57], the identification of these $\hat{\Pi}_i$ as combinations of the $\tilde{\Pi}_i$ is straightforward.



Figure 2. Two examples of the two-loop perturbative topologies. The external static photon has been indicated by a crossed vertex.

which employs a Laporta algorithm to reach a minimal set of master integrals. Explicit analytic expressions of the master integrals can be found in the literature.

The gluonic corrections to the quark loop are obtained by including two quark-gluon vertices from the Dyson series expansion in (2.1), i.e.

$$\begin{aligned} \Pi^{\mu_1\mu_2\mu_3\mu_4} &= -i \int \frac{d^4 q_3}{(2\pi)^4} \left(\prod_{i=1}^4 \int d^4 x_i e^{-iq_i x_i} \right) \\ &\times \langle 0|T \left(\prod_{j=1}^4 J^{\mu_j}(x_j) \frac{1}{2} \int d^4 z_1 d^4 z_2 i\mathcal{L}_{\text{int}}^{\text{qgq}}(z_1) i\mathcal{L}_{\text{int}}^{\text{qgq}}(z_2) \right) |0\rangle. \end{aligned} \quad (3.1)$$

Denoting colour indices with bars, the interaction Lagrangians above are of the form

$$\mathcal{L}_{\text{int}}^{\text{qgq}}(z_i) = g_S \frac{\lambda^{a_i}}{2} \bar{\gamma}_i^{\bar{\delta}_i} B_{\nu_i}^{a_i}(z_i) \bar{q}^{\bar{\nu}_i}(z_i) \gamma^{\nu_i} q^{\delta_i}(z_i), \quad (3.2)$$

where $B_{\nu_i}^{a_i}$ is the gluon field, g_S is the strong coupling and λ^{a_i} is an $SU(3)_c$ Gell-Mann matrix. The only nonzero topology at this order is obtained by connecting all the quarks to the same line. Two examples of the diagrams in question are shown in figure 2. As a consequence of the topology, both the quark electric charge e_q^4 and the colour factor, $\text{Tr}(\lambda^a \lambda^b) \delta_{ab} = 2(N_c^2 - 1)$, can be factored out, allowing to re-express the total contribution as a sum of all possible hexagons where two of the external lines are to be contracted to form the second loop, i.e.,

$$\Pi^{\mu_1\mu_2\mu_3\mu_4} = \frac{(N_c^2 - 1)g_s^2 e_q^4}{4} \int \frac{d^4 q_5}{(2\pi)^4} \frac{g_{\mu_5\mu_6}}{q_5^2} \lim_{q_6 \rightarrow -q_5} H^{\mu_1\mu_2\mu_3\mu_4\mu_5\mu_6}, \quad (3.3)$$

where

$$\begin{aligned} H^{\mu_1\mu_2\mu_3\mu_4\mu_5\mu_6} &\equiv \int \frac{d^4 p}{(2\pi)^4} \sum_{\sigma(1,2,4,5,6)} \text{Tr} \left(\gamma^{\mu_3} S(p+q_1+q_2+q_4+q_5+q_6) \gamma^{\mu_1} S(p+q_2+q_4+q_5+q_6) \right. \\ &\quad \left. \times \gamma^{\mu_2} S(p+q_4+q_5+q_6) \gamma^{\mu_4} S(p+q_5+q_6) \gamma^{\mu_5} S(p+q_6) \gamma^{\mu_6} S(p) \right). \end{aligned} \quad (3.4)$$

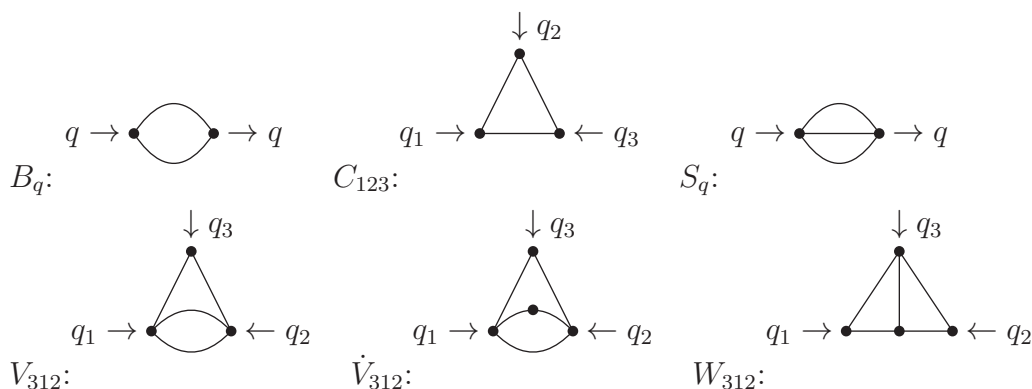


Figure 3. Master integrals appearing in the two-loop calculation. The dot on the propagator in \dot{V}_{312} corresponds to a doubling of that propagator.

Here, $S(p) = \frac{\not{p}}{p^2}$ is the massless quark propagator and $\sigma(1, 2, 4, 5, 6)$ the set of pairwise permutations of μ_i and q_i for $i = 1, 2, 3, 5, 6$. The corresponding $\tilde{\Pi}_i$ for the two loops are

$$\begin{aligned} \tilde{\Pi}_i &= P_{\mu_1\mu_2\mu_3\mu_4\nu_4}^{\tilde{\Pi}_i} \lim_{q_4 \rightarrow 0} \frac{\partial \Pi^{\mu_1\mu_2\mu_3\nu_4}}{\partial q_4^{\mu_4}} \\ &= -\frac{(N_c^2 - 1)g_s^2 e^4}{4} \int \frac{d^4 q_5}{(2\pi)^4} \frac{g_{\mu_5\mu_6}}{q_5^2} \lim_{\substack{q_4 \rightarrow 0 \\ q_6 \rightarrow -q_5}} P_{\mu_1\mu_2\mu_3\mu_4\nu_4}^{\tilde{\Pi}_i} \frac{\partial}{\partial q_4^{\nu_4}} H^{\mu_1\mu_2\mu_3\mu_4\mu_5\mu_6}. \end{aligned} \quad (3.5)$$

After taking the derivative, using

$$\frac{\partial}{\partial q_4^{\nu_4}} S(p + q_4) = -S(p + q_4) \gamma_{\nu_4} S(p + q_4), \quad (3.6)$$

the limit $q_4 \rightarrow 0$ and the projectors, we have for every $\tilde{\Pi}_i$ a large set of scalar two-loop integrals depending on two external momenta, q_1 , and q_2 , which can be parametrized as

$$\begin{aligned} M(i_1, \dots, i_7) &= \frac{1}{i^2} \int \frac{d^d p_1}{(2\pi)^d} \int \frac{d^d p_2}{(2\pi)^d} \\ &\quad \times \frac{1}{p_1^{2i_1} (p_1 - q_1)^{2i_2} (p_1 + q_2)^{2i_3} p_2^{2i_4} (p_2 - q_1)^{2i_5} (p_2 + q_2)^{2i_6} (p_1 - p_2)^{2i_7}}. \end{aligned} \quad (3.7)$$

Using KIRA [60] they can be reduced to the ones in table 1, whose corresponding topologies are represented in figure 3. This reduction is done in $d = 4 - 2\epsilon \neq 4$ dimensions.

This is a good point to discuss how we handle renormalization and regularization. Both ultraviolet and infrared divergences are regulated using dimensional regularization. We work to the lowest order in α and to first order in α_S in the massless quark limit. There are no counterterms needed to this order and infrared divergences must vanish since the three photon amplitude vanishes because of charge-conjugation. However, individual diagrams and master integral can be infrared and ultraviolet divergent. The quantities $\tilde{\Pi}_i$ are finite and the cancellation of all divergences, up to $1/\epsilon^3$ provides another good check on our calculations.

Strong efforts have been made to successfully obtain compact analytical expressions for all those two-loop integrals. All of the appearing master integrals can be found in

i_1, \dots, i_7	$M(i_1, \dots, i_7)$
1, 1, 0, 1, 1, 0, 0	B_1^2
1, 0, 1, 1, 0, 1, 0	B_2^2
0, 1, 1, 0, 1, 1, 0	B_3^2
1, 0, 1, 1, 1, 0, 0	$B_1 B_2$
0, 1, 1, 1, 1, 0, 0	$B_1 B_3$
0, 1, 1, 1, 0, 1, 0	$B_2 B_3$
1, 1, 1, 1, 1, 0, 0	$B_1 C_{123}$
1, 1, 1, 1, 0, 1, 0	$B_2 C_{123}$
1, 1, 1, 0, 1, 1, 0	$B_3 C_{123}$
0, 1, 0, 1, 0, 0, 1	S_1
0, 0, 1, 1, 0, 0, 1	S_2
0, 0, 1, 0, 1, 0, 1	S_3
0, 0, 1, 1, 1, 0, 1	V_{123}
0, 0, 1, 1, 1, 0, 2	\dot{V}_{123}
1, 0, 1, 0, 1, 0, 1	V_{213}
1, 0, 1, 0, 1, 0, 2	\dot{V}_{213}
0, 1, 1, 1, 0, 0, 1	V_{312}
0, 1, 1, 1, 0, 0, 2	\dot{V}_{312}
0, 1, 1, 1, 0, 1, 1	W_{123}
0, 1, 1, 1, 1, 0, 1	W_{213}
1, 0, 1, 1, 1, 0, 1	W_{312}
1, 1, 1, 1, 1, 1, 0	C_{123}^2

Table 1. List of master integrals $M(i_1, \dots, i_7)$ needed for the massless fully off-shell triangle at two-loop order. The last one is not needed at this order.

terms of classical polylogarithms in refs. [61, 62] up to the order that we need. They are collected together with their corresponding ϵ expansions in appendix A. Using these we find, as expected, that all the intermediate divergences exactly cancel, leading to a result of the following form

$$\begin{aligned}
 \tilde{\Pi}_m = & f_{m,ijk}^{pqr} F_{ijk}(2) Q_1^{2p} Q_2^{2q} Q_3^{2r} + w_{m,ijk}^{pqr} W_{ijk}(0) Q_1^{2p} Q_2^{2q} Q_3^{2r} + c_{m,ijk}^{pqr} C_{ijk}(0) Q_1^{2p} Q_2^{2q} Q_3^{2r} \\
 & + n_{m,1}^{pqr} Q_1^{2p} Q_2^{2q} Q_3^{2r} \log \frac{Q_1^2}{Q_3^2} + n_{m,2}^{pqr} Q_1^{2p} Q_2^{2q} Q_3^{2r} C_{ijk}(0) \log \frac{Q_2^2}{Q_3^2} \\
 & + l_{m,ijk1}^{pqr} Q_1^{2p} Q_2^{2q} Q_3^{2r} C_{ijk}(0) \log \frac{Q_1^2}{Q_3^2} + l_{m,ijk2}^{pqr} Q_1^{2p} Q_2^{2q} Q_3^{2r} C_{ijk}(0) \log \frac{Q_2^2}{Q_3^2}. \quad (3.8)
 \end{aligned}$$

The remaining loop functions, $C_{ijk}(0), W_{ijk}(0), F_{ijk}(2)$ can also be found in appendix A.

	$\tilde{\Pi}_1$	$\tilde{\Pi}_7$	$\tilde{\Pi}_{10}$	$\tilde{\Pi}_{13}$	$\tilde{\Pi}_{19}$
Quark loop	-0.0816	0.123	0.0363	0.0274	0.0263
Gluon corrections ($\times\pi/\alpha_s$)	0.0781	-0.136	-0.0376	-0.0398	-0.0411

Table 2. Values for the quark loop and gluonic correction contributions to the $\tilde{\Pi}$ in GeV units for a benchmark tuple $(Q_1^2, Q_2^2, Q_3^2) = (1, 1.3, 1.7) \text{ GeV}^2$. Sum over the three flavours has been made. The last line is in units of α_s/π .

	$\hat{\Pi}_1$	$\hat{\Pi}_4$	$\hat{\Pi}_7$	$\hat{\Pi}_{17}$	$\hat{\Pi}_{39}$	$\hat{\Pi}_{54}$
Quark loop	-0.0210	-0.0119	-0.00384	0.00386	0.0119	0.000422
Gluon corrections ($\times\pi/\alpha_s$)	0.0178	0.00560	0.00302	-0.00750	-0.0103	-0.000427

Table 3. Values for the quark loop and gluonic correction contributions to the $\hat{\Pi}$ in GeV units for a benchmark tuple $(Q_1^2, Q_2^2, Q_3^2) = (1, 1.3, 1.7) \text{ GeV}^2$. Sum over the three flavours has been made. The last line is in units of α_s/π .

The explicit numerical coefficients can be found in the file `pitildes.txt` of the supplementary material. In table 2 we give numerical results for them in a benchmark point, $(Q_1^2, Q_2^2, Q_3^2) = (1, 1.3, 1.7) \text{ GeV}^2$, giving also the analogous quark loop ones for comparison. The loop corrections are found of the order of $\sim -\frac{\alpha_s}{\pi}$, i.e. they are found to be small as far as α_s is not large. The scale at which α_s should be set is similar to the scale Q^2 at which the $\tilde{\Pi}$ are evaluated. Otherwise, large logarithms $\ln \frac{\mu}{Q_i}$ appearing at higher orders would break the perturbative series. As a consequence, the series are found to be reliable as far as we do not go below $\sim 1 \text{ GeV}$.

Taking the linear combinations of the $\tilde{\Pi}_i$ which lead to the $\hat{\Pi}$, one finds analogous expressions for them, but with explicit negative powers of Källén functions $\lambda = (Q_1^2 + Q_2^2 - Q_3^2)^2 - 4Q_1^2Q_2^2$. They introduce singularities which are, however, spurious. When expanding around them, they cancel against the zeros of the polylogarithms, as explicitly checked in different kinematic limits. Details on these expansions can be found in appendix A. Numerical values for the $\hat{\Pi}_i$ in the same benchmark point and comparison with the corresponding quark loop are given in table 3. The analytical expressions are too long to be included here and are given in the file `resultsgluon.txt` of the supplementary material. The equivalent results for the massless quark loop are in the file `resultsquark.txt`. We have, however, included analytical expressions for both the quark loop and gluonic correction at the symmetric point $Q_1 = Q_2 = Q_3$ in appendix B.

A possible check on our result is taking the limit where one of the virtualities is much smaller than the other two, i.e. the limit of ref. [45], where it is argued that the leading term should have no corrections. The consequences of this limit for the $\hat{\Pi}_i$ has been analyzed in ref. [36], where it is shown that only for $\hat{\Pi}_1$ there is an unambiguous prediction. Taking into account the corrections to the OPE of two-photon currents to the axial current, i.e. the axial current gets an extra factor of $1 - \alpha_S/\pi$ [51, 63–65], we see that our result indeed satisfies the arguments of ref. [45].

	Quark loop	Gluon corrections ($\frac{\alpha_s}{\pi}$ units)
$\bar{\Pi}_1$	0.0084	-0.0077
$\bar{\Pi}_2$	13.28	-12.30
$\bar{\Pi}_3$	0.78	-0.87
$\bar{\Pi}_4$	-2.25	0.62
$\bar{\Pi}_5$	0.00	0.20
$\bar{\Pi}_6$	2.34	-1.43
$\bar{\Pi}_7$	-0.097	0.056
$\bar{\Pi}_8$	0.035	0.41
$\bar{\Pi}_9$	0.623	-0.87
$\bar{\Pi}_{10}$	1.72	-1.61
$\bar{\Pi}_{11}$	0.696	-1.04
$\bar{\Pi}_{12}$	0.165	-0.16
Total	17.3	-17.0

Table 4. Leading contributions to the $(g - 2)_\mu$ integration from $Q_{\min} = 1$ GeV in 10^{-11} units.

4 Results for the $(g - 2)_\mu$ and phenomenological implications

Now that we have the needed gluonic corrections to the $\hat{\Pi}_i$, we can introduce them into (2.34) to calculate their corresponding contributions to a_μ^{HLbL} . Obviously, the identification of the $\hat{\Pi}_i$ with the ones obtained using the OPE only makes sense when such an expansion is valid, i.e., above some cut for the Euclidean momenta, $Q_{1,2,3} > Q_{\min}$. We restrict ourselves to those integration regions, keeping in mind that the (dominant) contributions from the remaining regions, necessarily computed with non-perturbative methods, must be added to the ones computed here.

The numerical integration has been done with the VEGAS implementation in the CUBA library, as well as our own implementation of two deterministic algorithms. We have checked that the results agree. The general expressions for the quark loop and the gluonic corrections have large negative powers of λ and become numerically unstable whenever λ is small. We therefore use, as in our previous work for the quark loop [57], expansions whenever that happens. There are six different expansions that need to be done. This is explained in more detail in appendix B. We have checked that the numerical results are not sensitive to changing the boundaries where we use the different expansions.

We perform the integrals of the $12\bar{\Pi}_i$ contributions at different Q_{\min} , both for the leading OPE contribution, the quark loop, and the gluonic corrections. They are displayed for $Q_{\min} = 1$ GeV in table 4.

Consistently with the size of the gluonic corrections found for the $\tilde{\Pi}_i$ in the previous section, we find that they are negative and of order $\frac{\alpha_s}{\pi}$. Given the power fall-off of the contributions of the $\hat{\Pi}$ with respect to the studied energies, the quantitative contri-

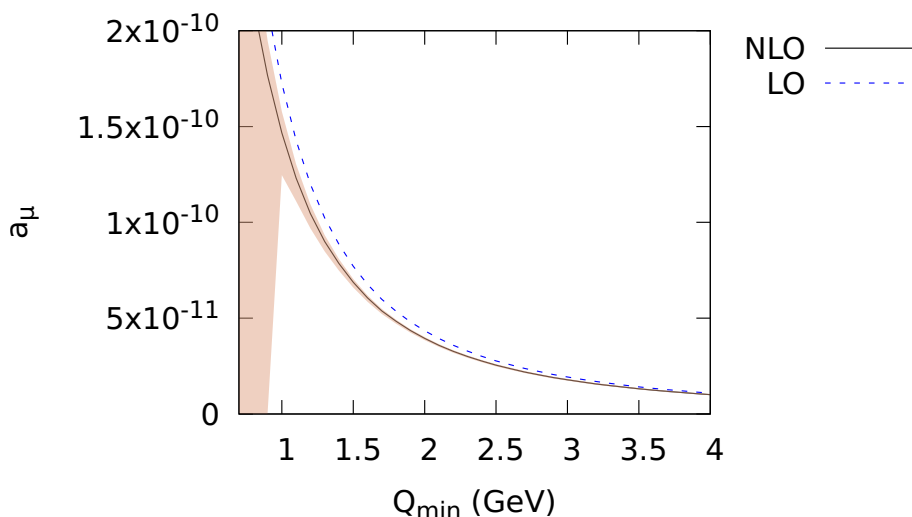


Figure 4. Numerical results for the hadronic HLbL $(g - 2)_\mu$ in the $Q_i > Q_{\min}$ region, using the LO (massless quark loop) and NLO (gluonic corrections) contributions of its corresponding OPE. Uncertainties, apart from the one coming from the $\alpha_s(M_W)$ input, represented by shaded areas have been estimated attending to ambiguities when setting the α_s input (exact choice of scale and order of running for the β function) as a consequence of not including higher-orders.

bution above some energy cut Q_{\min} is saturated by the regions nearby such a cut. As a consequence, a natural scale to effectively avoid large logarithms in the corresponding perturbative series is $\mu \sim Q_{\min}$, however the exact choice of it is ambiguous. In order to estimate perturbative uncertainties we will vary the scale dependence, a consequence of cutting the series at two-loops or at the first α_S correction, in the interval $\mu^2 \in (\frac{1}{2}, 2)Q_{\min}^2$. At the studied order, the whole scale dependence comes from $\alpha_s(\mu)$. Taking $\alpha_s^{N_f=5}(M_Z)$ from ref. [66], we run it at five loops to $\alpha_s^{N_f=3}(m_\tau)$.³ As a further conservative estimates of perturbative uncertainty, we add quadratically the difference obtained by taking the one obtained running from $\alpha_s^{N_f=3}(m_\tau)$ to $\alpha_s^{N_f=3}(Q_{\min})$ with the five loop running (which we take as our central result) with the one obtained keeping $\alpha_s^{N_f=3}$ with a fixed scale, $\mu = m_\tau$, which at the order we are working with is also a legitimate choice. Finally we also add quadratically the subleading uncertainty coming from $\alpha_s^{N_f=5}(M_Z)$.

The result, where we show the quark loop, the gluonic corrections and the obtained uncertainties is shown in figure 4. While in general we consider our uncertainty estimates reliable, we notice that they may be slightly over-conservative in the region just below 1 GeV and over-optimistic just above it. This is a consequence of the sharp break down of the α_s running at $\mu \sim 0.7$ GeV which makes our uncertainty strongly dependent on the exact scale interval chosen to estimate them. In essence, we find that the correction is small and negative and that the series are well-behaved, having a gluonic correction of around -10% above the perturbative breakdown.

³We implement the running, in the conventional $\overline{\text{MS}}$ scheme, using RUNDEC [67].

5 Conclusions

One of the main sources of uncertainties entering in $(g - 2)_\mu$ comes from the contributions of the short-distance regions of the HLbL tensor contributions. In this work, which can be regarded as a continuation of refs. [54] and [57], we have culminated our task of giving a precise and systematic description of the contributions for three large loop momenta.

For years, it was assumed that some form of the quark loop, maybe with constituent quark masses, should be the leading order of some systematic expansion of the HLbL contribution tensor to the $(g - 2)_\mu$ for large loop momenta. However, it was shown in ref. [54] how applying an OPE directly to the HLbL tensor, where the massless quark loop is indeed the leading order, does not make sense for the $(g - 2)_\mu$ kinematics. The correct expansion in this kinematic region was presented in that reference, where the massless quark loop was shown to be the leading order and the leading non-perturbative quark mass-suppressed correction was computed.

A very comprehensive analysis to study the role of both the quark mass-suppressed and not suppressed non-perturbative corrections to the expansion was made in ref. [57], where many formal aspects and subtleties of the expansion were developed and presented in full detail, showing that it is well founded. The obtained results showed how above 1 GeV the non-perturbative corrections, even when functionally more important than in other expansions, are still typically below 1%.

In view of that, the most important corrections to the leading massless quark loop, and the one that ultimately allows to understand from where the expansion is valid, is the pure gluonic correction, which has been the subject of this work.

While in principle a multi-scale four-loop integral could be regarded as a formidable task, it has become feasible through combining existing tools developed for generic contributions of the HLbL tensor to the $(g - 2)_\mu$, methods on finding compact expressions developed in ref. [57], optimized software on reduction to master integrals, analytic reduction of those remaining master integrals and numerical integration routines.

Our final result brings good news. The size of the gluonic corrections are found small, typically of size -10% above the perturbative breakdown scale, and, as a consequence, the expansion is able to give a precise description of the $(g - 2)_\mu$ contributions above it.

Taking all of this into account, we suggest as a legitimate method to compute the HLbL contribution to $(g - 2)_\mu$ to use the results of this expansion from some point between $Q_{\min} = 1 \text{ GeV}$ and $Q_{\min} = 2 \text{ GeV}$, which should give a more precise prediction than resonance models, and possible discontinuities in the matching should be incorporated as systematic model uncertainty.

Acknowledgments

We thank Martin Hoferichter for discussions. N. H.-T. and L.L. are funded by the Albert Einstein Center for Fundamental Physics at Universität Bern and the Swiss National Science Foundation, respectively. J. B. is supported in part by the Swedish Research Council grants contract numbers 2016-05996 and 2019-03779. A. R.-S. is partially supported by the Agence Nationale de la Recherche (ANR) under grant ANR-19-CE31-0012 (project MORA).

A Master integrals

The aim of this appendix is to list the expressions of the master integrals needed in section 3 (see also figure 3). They can be found in refs. [61, 62, 68].⁴ All n-loop master integrals contain the overall factor S_D^n , where

$$S_D = S_D(\epsilon) = \frac{(4\pi)^\epsilon \Gamma(1 + \epsilon) \Gamma^2(1 - \epsilon)}{16\pi^2 \Gamma(1 - 2\epsilon)}. \quad (\text{A.1})$$

The functions C_{123} and W_{312} are finite in the limit $d \rightarrow 4$. Their ϵ -expansions can be written as follows

$$\begin{aligned} C_{123} &\equiv \int dp \frac{1}{p^{2\gamma}(p - q_1)^2(p + q_2)^2} \\ &= S_D C_{123}(0) + S_D C_{123}(1)\epsilon + C_{123}(2)\epsilon^2 + \mathcal{O}(\epsilon^3), \end{aligned} \quad (\text{A.2})$$

$$\begin{aligned} W_{312} &\equiv \int dp_1 dp_2 \frac{1}{p_1^2(p_1 + q_2)^2 p_2^2(p_2 - q_1)^2(p_1 - p_2)^2} \\ &= S_D^2 W_{312}(0) + S_D^2 W_{312}(1)\epsilon + W_{312}(2)\epsilon^2 + \mathcal{O}(\epsilon^2), \end{aligned} \quad (\text{A.3})$$

where $q_1 + q_2 + q_3 = 0$ and $d = 4 - 2\epsilon$. The integrations are defined as

$$\int dp = \frac{1}{i} \int \frac{d^d p}{(2\pi)^d}. \quad (\text{A.4})$$

The remaining integrals appearing in the calculation contain some singularities which cancel out in the final amplitude. The ϵ -expansions of the integral B_q and S_q read

$$\begin{aligned} B_q &\equiv \int dp \frac{1}{p^2(p - q)^2} \\ &= \frac{S_D}{\epsilon} + S_D \left[2 - \log(-q^2) \right] + S_D \left[4 - 2 \log(-q^2) + \frac{1}{2} \log^2(-q^2) \right] \epsilon + \mathcal{O}(\epsilon^2), \end{aligned} \quad (\text{A.5})$$

and

$$\begin{aligned} S_q &\equiv \int dp_1 dp_2 \frac{1}{(p_1 - q)^2 p_2^2 (p_1 - p_2)^2} \\ &= -S_D^2 \frac{q^2}{4\epsilon} + S_D^2 \left[-\frac{13}{8} q^2 + \frac{1}{2} \log(-q^2) q^2 \right] \\ &\quad + S_D^2 \left[-\frac{115}{16} q^2 + \frac{13}{4} \log(-q^2) q^2 - \frac{1}{2} \log^2(-q^2) q^2 \right] \epsilon + \mathcal{O}(\epsilon^2). \end{aligned} \quad (\text{A.6})$$

⁴The formulas given in this appendix and those in ref. [62] differ in a sign: an overall minus sign has been missed in (4.18) of ref. [62]. This in turns leads to a minus instead of the plus sign in the second line of (4.24), which corresponds to our (A.7). We checked that our sign agrees with the corresponding formulas in ref. [68], which is also cited in ref. [62].

The integrals V_{123} and \dot{V}_{123} can be expressed as functions of the finite integrals C_{123} and W_{312} . Their ϵ -expansions can be written as

$$\begin{aligned} \dot{V}_{312} &\equiv \int dp_1 dp_2 \frac{1}{p_1^2(p_1 - q_1)^2(p_1 + q_2)^2 p_2^2(p_1 - p_2)^2} \\ &= -S_D^2 \frac{C_{123}(0)}{\epsilon} + S_D^2 \left[\frac{1}{2} C_{123}(0) \left(\log(-q_1^2) + \log(-q_2^2) \right) - C_{123}(1) \right] \\ &\quad - \frac{S_D^2}{4} \left[C_{123}(0) \left(\log^2(-q_1^2) + \log^2(-q_2^2) \right) - 2C_{123}(1) \left(\log(-q_1^2) + \log(-q_2^2) \right) \right. \\ &\quad \left. + 4(C_{123}(2) + W_{312}(0)) \right] \epsilon + \mathcal{O}(\epsilon^2), \end{aligned} \tag{A.7}$$

and

$$\begin{aligned} V_{312} &\equiv \int dp_1 dp_2 \frac{1}{(p_1 - q_1)^2(p_1 + q_2)^2 p_2^2(p_1 - p_2)^2} \\ &= \frac{S_D^2}{2\epsilon^2} + S_D^2 \left[\frac{5}{2} - \log(-q_3^2) \right] \frac{1}{\epsilon} + \frac{S_D^2}{2} \left[C_{123}(0)(-q_1^2 - q_2^2 + q_3^2) \right. \\ &\quad \left. + \log(-q_1^2) \left(\log(-q_3^2) - \log(-q_2^2) \right) + \log(-q_2^2) \log(-q_3^2) + \log^2(-q_3^2) - 10\log(-q_3^2) + 19 \right] \\ &\quad + S_D^2 \left[\frac{1}{2} (F_{312}(2) + 65) + \frac{1}{2} C_{123}(1)(-q_1^2 - q_2^2 + q_3^2) \right. \\ &\quad \left. + C_{123}(0) \left(-\frac{5}{2}(q_1^2 + q_2^2 - q_3^2) + \frac{1}{4} \log(-q_1^2)(q_1^2 + q_2^2 - q_3^2) + \frac{1}{4} \log(-q_2^2)(q_1^2 + q_2^2 - q_3^2) \right) \right. \\ &\quad \left. + \log(-q_1^2) \left(\log(-q_2^2) \left(\log(-q_3^2) - \frac{5}{2} \right) - \log^2(-q_3^2) + \frac{5\log(-q_3^2)}{2} \right) \right. \\ &\quad \left. + \log(-q_2^2) \left(\frac{5\log(-q_3^2)}{2} - \log^2(-q_3^2) \right) + \frac{1}{3} \log^3(-q_3^2) + \frac{5}{2} \log^2(-q_3^2) - 19\log(-q_3^2) \right] \epsilon \\ &\quad + \mathcal{O}(\epsilon^2), \end{aligned} \tag{A.8}$$

where $C_{123}(i)$ and $W_{312}(i)$ are the coefficients of the ϵ -expansion of their corresponding Master integral (cf. (A.2) and (A.3)). Not all these coefficients survive in the gluonic corrections we are computing in section 3: $C_{123}(1)$, $C_{123}(2)$, $W_{312}(1)$ and $W_{312}(2)$ cancel in the final expression. The coefficients $C_{123}(0)$ and $W_{312}(0)$ that contribute, as well as the function $F_{312}(2)$ which appears in the expansion of V_{312} , are given below

$$C_{123}(0) = 2q_3^{-2} \frac{\mathcal{P}_2(z)}{z - \bar{z}}, \tag{A.9}$$

$$W_{312}(0) = 6q_3^{-2} \frac{\mathcal{P}_4(1 - z^{-1})}{z - \bar{z}}, \tag{A.10}$$

and finally

$$F_{312}(2) = -6\mathcal{P}_3(z) - 6\mathcal{P}_3(1 - z) + \frac{1}{2} \log(u) \log^2(v) + \frac{1}{2} \log^2(u) \log(v) + 6\zeta_3, \tag{A.11}$$

where $u = \frac{q_1^2}{q_3^2}$, $v = \frac{q_2^2}{q_3^2}$ and z is given by

$$\begin{aligned} z &= \frac{1}{2} \left(1 + u - v + i\sqrt{-\bar{\lambda}} \right), \\ \bar{\lambda} &= (1 + u - v)^2 - 4u. \end{aligned} \tag{A.12}$$

The $\mathcal{P}_i(z)$ are real (purely imaginary) functions over the complex plane when i is odd (real). They can be expressed using polylogarithms:

$$\begin{aligned}
 \mathcal{P}_2(z) &= \text{Li}_2(z) - \text{Li}_2(\bar{z}) + \log|z|(\log(1-z) - \log(1-\bar{z})) \\
 \mathcal{P}_3(z) &= \text{Li}_3(z) + \text{Li}_3(\bar{z}) - \log|z|(\text{Li}_2(z) + \text{Li}_2(\bar{z})) - \frac{1}{3} \log^2|z|(\log(1-z) + \log(1-\bar{z})) \\
 \mathcal{P}_4(z) &= \text{Li}_4(z) - \text{Li}_4(\bar{z}) - \log|z|(\text{Li}_3(z) - \text{Li}_3(\bar{z})) + \frac{1}{3} \log^2|z|(\text{Li}_2(z) - \text{Li}_2(\bar{z})) \quad (\text{A.13})
 \end{aligned}$$

The polylogarithms can be defined recursively

$$\text{Li}_n(z) = \int_0^z \frac{dt}{t} \text{Li}_{n-1}(t), \text{ and } \text{Li}_1(z) = -\log(1-z). \quad (\text{A.14})$$

The \mathcal{P}_i satisfy a number of relations

$$\begin{aligned}
 \mathcal{P}_2(z) &= -\mathcal{P}_2(1/z), \\
 \mathcal{P}_3(z) &= \mathcal{P}_3(1/z), \\
 \mathcal{P}_4(z) &= -\mathcal{P}_4(1/z), \\
 \mathcal{P}_2(z) &= \mathcal{P}_2(1-1/z) = -\mathcal{P}_2(1-z) = \mathcal{P}_2(1/(1-z)) = -\mathcal{P}_2(z/(z-1)), \\
 \mathcal{P}_3(z) + \mathcal{P}_3(1-z) + \mathcal{P}_3(1-1/z) &= \mathcal{P}_3(1) = 2\zeta(3) \quad (\text{A.15})
 \end{aligned}$$

which can be used to show that the master integrals have the required symmetries under interchange of momenta.

B Analytical formulae

In this section we present analytical formulae for the scalar functions entering into the calculation of a_μ^{HLbL} . We in particular discuss the momentum expansions of the master integrals needed to make spurious singularities cancel numerically. As an explicit example, we also give the expressions for the $\hat{\Pi}$ at the symmetric point $Q_1 = Q_2 = Q_3$ for the quark loop and gluonic correction in appendix B.2.

B.1 Expansions

In the numerical evaluation of a_μ^{HLbL} there are certain limits of the kinematics requiring particular care. The integration domain can be divided into several regions as in figure 5. We there see the so-called side, corner and inside regions together with their boundaries. Also the cut-off μ has been indicated. Unless the side and corner regions are properly taken care of, the numerical integration will diverge as one obtains zeros in denominators that numerically do not cancel the zeros in numerators. Below we discuss the two types of problematic regions.

The precise definition of the regions is: $Q_i \geq \mu = Q_{\min}$. The corners are defined by $Q_i/(Q_1 + Q_2 + Q_3) \leq \epsilon_1$ for $i = 1, 2, 3$. The sides are the part of the remaining region that satisfy $(2Q_i/(Q_1 + Q_2 + Q_3) - 1) \leq \epsilon_2$ for $i = 1, 2, 3$. The inside is the remaining allowed region.

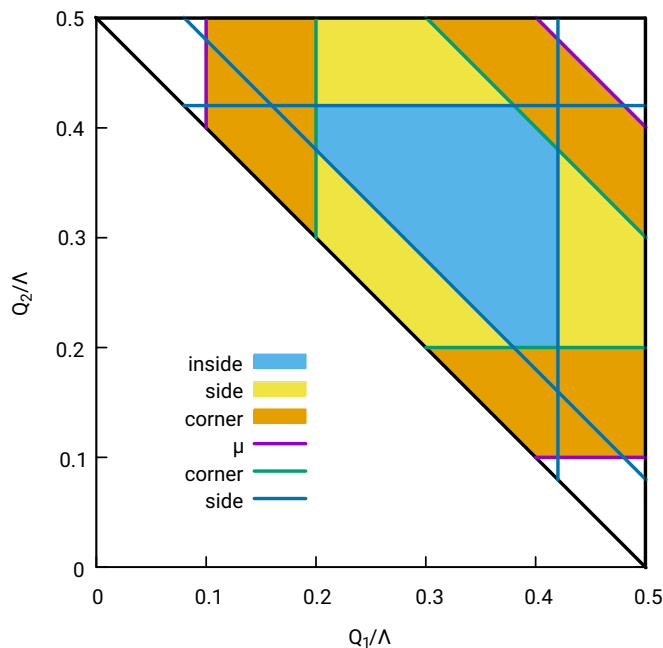


Figure 5. Different regions to consider in order to deal with the singularities of the $\hat{\Pi}$ when $\lambda \rightarrow 0$. The regions are shown for $Q_1 + Q_2 + Q_3 = \Lambda$.

B.1.1 Side regions

The side regions are defined as the kinematical limit where one Q_i is close to $Q_j + Q_k$, or, in other words when

$$\text{Side Region } S_i : \quad Q_i^2 = (Q_j + Q_k)^2 - \delta \equiv \bar{Q}_i^2 - \delta, \quad (\text{B.1})$$

where δ is a small parameter. The inverse powers of the Källén function in the $\hat{\Pi}_i$ diverge in the side regions. These apparent singularities do, however, cancel when all the kinematical factors, the master integrals $C_{123}(0)$, $W_{312}(0)$, $W_{213}(0)$, $W_{123}(0)$, $F_{312}(2)$, $F_{213}(2)$ and $F_{123}(2)$ as well as the Källén function itself are expanded in δ . For a finite result we have to expand the master integrals up to order δ^9 . The analytical forms of these expansions are very long and we here therefore only give the first two orders for one case, S_3 . In the supplementary material file `sideexpansions.txt`, however, we provide the full expansions needed for all S_i . In region S_{+3} we have

$$\begin{aligned} C_{123}(0) &= \frac{1}{Q_2 Q_3} \log\left(\frac{Q_1^2}{Q_3^2}\right) + \frac{1}{Q_1 Q_3} \log\left(\frac{Q_2^2}{Q_3^2}\right) \\ &+ \delta \left[\frac{Q_1}{6Q_2^2 Q_3} \log\left(\frac{Q_1^2}{Q_3^2}\right) + \frac{Q_2}{6Q_1^2 Q_3} \log\left(\frac{Q_2^2}{Q_3^2}\right) + \frac{1}{3Q_2 Q_3} + \frac{1}{2Q_1 Q_3} \log\left(\frac{Q_1^2}{Q_3^2}\right) \right. \\ &\left. + \frac{1}{3Q_1 Q_3} + \frac{1}{2Q_1 Q_3} \log\left(\frac{Q_2^2}{Q_3^2}\right) \right] + \mathcal{O}(\delta^2), \end{aligned} \quad (\text{B.2})$$

$$\begin{aligned}
F_{312}(2) = & -6\zeta_3 + \frac{1}{2} \log\left(\frac{Q_1^2}{Q_3^2}\right) \log^2\left(\frac{Q_2^2}{Q_3^2}\right) + \frac{1}{2} \log^2\left(\frac{Q_1^2}{Q_3^2}\right) \log\left(\frac{Q_2^2}{Q_3^2}\right) + 6\mathcal{P}_3\left(-\frac{Q_2}{Q_1}\right) \\
& + \delta \left[-\frac{Q_2}{Q_1 Q_3^2} \log^2\left(\frac{Q_2^2}{Q_3^2}\right) - \frac{Q_2}{Q_1 Q_3^2} \log\left(\frac{Q_1^2}{Q_3^2}\right) \log\left(\frac{Q_2^2}{Q_3^2}\right) - \frac{Q_2}{Q_1 Q_3^2} \log^2\left(\frac{Q_1^2}{Q_3^2}\right) \right. \\
& - \frac{3}{Q_1 Q_3} \log\left(\frac{Q_2^2}{Q_3^2}\right) + \frac{1}{Q_1 Q_3} \log^2\left(\frac{Q_2^2}{Q_3^2}\right) + \frac{3}{Q_1 Q_3} \log\left(\frac{Q_1^2}{Q_3^2}\right) \\
& \left. + \frac{1}{Q_1 Q_3} \log\left(\frac{Q_1^2}{Q_3^2}\right) \log\left(\frac{Q_2^2}{Q_3^2}\right) + \frac{1}{Q_1 Q_3} \log^2\left(\frac{Q_1^2}{Q_3^2}\right) - \frac{3}{Q_1 Q_2} \log\left(\frac{Q_1^2}{Q_3^2}\right) \right] \\
& + \mathcal{O}(\delta^2), \tag{B.3}
\end{aligned}$$

$$\begin{aligned}
W_{312}(0) = & \frac{3}{Q_1 Q_2} \mathcal{P}_3\left(-\frac{Q_2}{Q_1}\right) \\
& + \delta \left[-\frac{1}{12 Q_1^2 Q_3^2} \log^2\left(\frac{Q_2^2}{Q_3^2}\right) + \frac{1}{6 Q_1^2 Q_3^2} \log\left(\frac{Q_1^2}{Q_3^2}\right) \log\left(\frac{Q_2^2}{Q_3^2}\right) - \frac{1}{12 Q_1^2 Q_3^2} \log^2\left(\frac{Q_1^2}{Q_3^2}\right) \right. \\
& - \frac{1}{2 Q_1^2 Q_2 Q_3} \log\left(\frac{Q_2^2}{Q_3^2}\right) + \frac{1}{12 Q_1^2 Q_2 Q_3} \log^2\left(\frac{Q_2^2}{Q_3^2}\right) + \frac{1}{2 Q_1^2 Q_2 Q_3} \log\left(\frac{Q_1^2}{Q_3^2}\right) \\
& - \frac{1}{6 Q_1^2 Q_2 Q_3} \log\left(\frac{Q_1^2}{Q_3^2}\right) \log\left(\frac{Q_2^2}{Q_3^2}\right) + \frac{1}{12 Q_1^2 Q_2 Q_3} \log^2\left(\frac{Q_1^2}{Q_3^2}\right) - \frac{1}{2 Q_1^2 Q_2^2} \log\left(\frac{Q_1^2}{Q_3^2}\right) \\
& \left. + \frac{1}{2 Q_1^2 Q_2^2} \mathcal{P}_3\left(-\frac{Q_2}{Q_1}\right) \right] + \mathcal{O}(\delta^2), \tag{B.4}
\end{aligned}$$

$$\begin{aligned}
F_{213}(2) = & -6\zeta_3 - \log^3\left(\frac{Q_2^2}{Q_3^2}\right) + \frac{3}{2} \log\left(\frac{Q_1^2}{Q_3^2}\right) \log^2\left(\frac{Q_2^2}{Q_3^2}\right) - \frac{1}{2} \log^2\left(\frac{Q_1^2}{Q_3^2}\right) \log\left(\frac{Q_2^2}{Q_3^2}\right) \\
& + 6\mathcal{P}_3\left(1 + \frac{Q_2}{Q_1}\right) + \delta \left[3 \frac{Q_2}{Q_1 Q_3^2} \log\left(\frac{Q_2^2}{Q_3^2}\right) + \frac{3 Q_2}{2 Q_1 Q_3^2} \log^2\left(\frac{Q_2^2}{Q_3^2}\right) \right. \\
& - \frac{3 Q_2}{Q_1 Q_3^2} \log\left(\frac{Q_1^2}{Q_3^2}\right) - \frac{5 Q_2}{2 Q_1 Q_3^2} \log\left(\frac{Q_1^2}{Q_3^2}\right) \log\left(\frac{Q_2^2}{Q_3^2}\right) + \frac{Q_2}{Q_1 Q_3^2} \log^2\left(\frac{Q_1^2}{Q_3^2}\right) \\
& - \frac{3}{2 Q_1 Q_3} \log^2\left(\frac{Q_2^2}{Q_3^2}\right) + \frac{3}{Q_1 Q_3} \log\left(\frac{Q_1^2}{Q_3^2}\right) + \frac{5}{2 Q_1 Q_3} \log\left(\frac{Q_1^2}{Q_3^2}\right) \log\left(\frac{Q_2^2}{Q_3^2}\right) \\
& \left. - \frac{1}{Q_1 Q_3} \log^2\left(\frac{Q_1^2}{Q_3^2}\right) \right] + \mathcal{O}(\delta^2), \tag{B.5}
\end{aligned}$$

$$\begin{aligned}
W_{213}(0) = & -\frac{3}{Q_1 Q_3} \mathcal{P}_3\left(1 + \frac{Q_2}{Q_1}\right) \\
& + \delta \left[-\frac{Q_2}{2 Q_1^2 Q_3^3} \log\left(\frac{Q_2^2}{Q_3^2}\right) + \frac{Q_2}{2 Q_1^2 Q_3^3} \log\left(\frac{Q_1^2}{Q_3^2}\right) + \frac{Q_2}{4 Q_1^2 Q_3^3} \log\left(\frac{Q_1^2}{Q_3^2}\right) \log\left(\frac{Q_2^2}{Q_3^2}\right) \right. \\
& \left. - \frac{Q_2}{4 Q_1^2 Q_3^3} \log^2\left(\frac{Q_1^2}{Q_3^2}\right) + \frac{Q_2}{Q_1^2 Q_3^3} \mathcal{P}_3\left(1 + \frac{Q_2}{Q_1}\right) - \frac{1}{2 Q_1^2 Q_3^2} \log\left(\frac{Q_1^2}{Q_3^2}\right) \right]
\end{aligned}$$

$$\begin{aligned}
& -\frac{1}{4Q_1^2\bar{Q}_3} \log\left(\frac{Q_1^2}{Q_3^2}\right) \log\left(\frac{Q_2^2}{Q_3^2}\right) + \frac{5}{12Q_1^2\bar{Q}_3} \log^2\left(\frac{Q_1^2}{Q_3^2}\right) - \frac{3}{2Q_1^2\bar{Q}_3} \mathcal{P}_3\left(1 + \frac{Q_2}{Q_1}\right) \\
& - \frac{1}{6Q_1^2Q_2\bar{Q}_3} \log^2\left(\frac{Q_1^2}{Q_3^2}\right) \Big] + \mathcal{O}(\delta^2), \tag{B.6}
\end{aligned}$$

$$\begin{aligned}
F_{123}(2) = & -6\zeta_3 - \frac{1}{2} \log\left(\frac{Q_1^2}{Q_3^2}\right) \log^2\left(\frac{Q_2^2}{Q_3^2}\right) + \frac{3}{2} \log^2\left(\frac{Q_1^2}{Q_3^2}\right) \log\left(\frac{Q_2^2}{Q_3^2}\right) - \log^3\left(\frac{Q_1^2}{Q_3^2}\right) \\
& + 6\mathcal{P}_3\left(1 + \frac{Q_1}{Q_2}\right) + \delta \left[-\frac{3Q_1}{Q_2Q_3} \log\left(\frac{Q_2^2}{Q_3^2}\right) + \frac{Q_1}{Q_2Q_3} \log^2\left(\frac{Q_2^2}{Q_3^2}\right) \right. \\
& + \frac{3Q_1}{Q_2Q_3} \log\left(\frac{Q_1^2}{Q_3^2}\right) - \frac{5Q_1}{2Q_2Q_3} \log\left(\frac{Q_1^2}{Q_3^2}\right) \log\left(\frac{Q_2^2}{Q_3^2}\right) + \frac{3Q_1}{2Q_2Q_3} \log^2\left(\frac{Q_1^2}{Q_3^2}\right) \\
& + \frac{3}{Q_2Q_3} \log\left(\frac{Q_2^2}{Q_3^2}\right) - \frac{1}{Q_2Q_3} \log^2\left(\frac{Q_2^2}{Q_3^2}\right) + \frac{5}{2Q_2Q_3} \log\left(\frac{Q_1^2}{Q_3^2}\right) \log\left(\frac{Q_2^2}{Q_3^2}\right) \\
& \left. - \frac{3}{2Q_2Q_3} \log^2\left(\frac{Q_1^2}{Q_3^2}\right) \right] + \mathcal{O}(\delta^2), \tag{B.7}
\end{aligned}$$

$$\begin{aligned}
W_{123}(0) = & -\frac{3}{Q_2Q_3} \mathcal{P}_3\left(1 + \frac{Q_1}{Q_2}\right) \\
& + \delta \left[\frac{Q_1}{2Q_2^2Q_3} \log\left(\frac{Q_2^2}{Q_3^2}\right) - \frac{Q_1}{4Q_2^2Q_3} \log^2\left(\frac{Q_2^2}{Q_3^2}\right) - \frac{Q_1}{2Q_2^2Q_3} \log\left(\frac{Q_1^2}{Q_3^2}\right) \right. \\
& + \frac{Q_1}{4Q_2^2Q_3} \log\left(\frac{Q_1^2}{Q_3^2}\right) \log\left(\frac{Q_2^2}{Q_3^2}\right) + \frac{Q_1}{Q_2^2Q_3} \mathcal{P}_3\left(1 + \frac{Q_1}{Q_2}\right) - \frac{1}{2Q_2^2Q_3} \log\left(\frac{Q_2^2}{Q_3^2}\right) \\
& + \frac{5}{12Q_2^2Q_3} \log^2\left(\frac{Q_2^2}{Q_3^2}\right) - \frac{1}{4Q_2^2Q_3} \log\left(\frac{Q_1^2}{Q_3^2}\right) \log\left(\frac{Q_2^2}{Q_3^2}\right) - \frac{3}{2Q_2^2Q_3} \mathcal{P}_3\left(1 + \frac{Q_1}{Q_2}\right) \\
& \left. - \frac{1}{6Q_1Q_2^2Q_3} \log^2\left(\frac{Q_2^2}{Q_3^2}\right) \right]. \tag{B.8}
\end{aligned}$$

To obtain these one has to expand the relevant \mathcal{P}_i functions around a general z . Note that one obtains e.g. $\mathcal{P}_3(1 + Q_2/Q_1)$, which, from the definition of the function in (A.13) gives rise to $\log(-Q_2/Q_1)$. This lies on the branch-cut of the (poly-)logarithm. However, the \mathcal{P}_i are well-behaved, single-valued functions without branch-cuts and one can safely neglect these issues.

When the $\hat{\Pi}$ are expanded, the negative powers of δ cancel. The expressions are not displayed here due to their length, but they can be found in the supplementary material file `resultsgluon.txt`. Equivalent expressions are provided for the quark loop in `resultsquark.txt`.

B.1.2 Corner regions

In the corner regions the situation is different. There one has two small parameters instead of one

$$\text{Corner Region } C_i : \quad Q_i \ll Q_j, Q_k \text{ and } \delta \equiv Q_j - Q_k \ll \bar{Q}_i \equiv Q_j + Q_k. \tag{B.9}$$

Below, we list the expansions in the region C_3 .⁵ The expansions of the master integrals are given by

$$C_{123}(0) = -\frac{8}{Q_3^2} + \frac{8}{Q_3^2} \log\left(2\frac{Q_3}{Q_3}\right) + Q_3^2 \left[-\frac{40}{9Q_3^4} + \frac{16}{3Q_3^4} \log\left(2\frac{Q_3}{Q_3}\right) \right] + \mathcal{O}\left(Q_3^4, \delta^2, \delta Q_3^2\right), \quad (\text{B.10})$$

$$W_{312}(0) = -\frac{24}{Q_3^2} \zeta_3 + Q_3^2 \left[\frac{88}{3Q_3^4} - \frac{16}{Q_3^4} \zeta_3 - \frac{16}{Q_3^4} \log\left(2\frac{Q_3}{Q_3}\right) \right] + \mathcal{O}\left(Q_3^4, \delta^2, \delta Q_3^2\right), \quad (\text{B.11})$$

$$F_{312}(2) = 6\zeta_3 - 8\log^3\left(2\frac{Q_3}{Q_3}\right) + Q_3^2 \left[-\frac{36}{Q_3^2} + \frac{24}{Q_3^2} \log\left(2\frac{Q_3}{Q_3}\right) \right] + \mathcal{O}\left(Q_3^4, \delta^2, \delta Q_3^2\right) \quad (\text{B.12})$$

$$\begin{aligned} W_{213}(0) = & -\frac{24}{Q_3^2} + \frac{24}{Q_3^2} \log\left(2\frac{Q_3}{Q_3}\right) - \frac{8}{Q_3^2} \log^2\left(2\frac{Q_3}{Q_3}\right) \\ & + Q_3^2 \left[-\frac{130}{27Q_3^4} + \frac{76}{9Q_3^4} \log\left(2\frac{Q_3}{Q_3}\right) - \frac{40}{9Q_3^4} \log^2\left(2\frac{Q_3}{Q_3}\right) \right] \\ & + \delta \left[\frac{18}{Q_3^3} - \frac{20}{Q_3^3} \log\left(2\frac{Q_3}{Q_3}\right) + \frac{8}{Q_3^3} \log^2\left(2\frac{Q_3}{Q_3}\right) \right] + \mathcal{O}\left(Q_3^4, \delta^2, \delta Q_3^2\right), \end{aligned} \quad (\text{B.13})$$

$$\begin{aligned} F_{213}(2) = & -6\zeta_3 + Q_3^2 \left[\frac{18}{Q_3^2} - \frac{12}{Q_3^2} \log\left(2\frac{Q_3}{Q_3}\right) \right] \\ & + \delta \left[\frac{24}{Q_3} - \frac{24}{Q_3} \log\left(2\frac{Q_3}{Q_3}\right) + \frac{16}{Q_3} \log^2\left(2\frac{Q_3}{Q_3}\right) \right] + \mathcal{O}\left(Q_3^4, \delta^2, \delta Q_3^2\right), \end{aligned} \quad (\text{B.14})$$

$$\begin{aligned} W_{123}(0) = & -\frac{24}{Q_3^2} + \frac{24}{Q_3^2} \log\left(2\frac{Q_3}{Q_3}\right) - \frac{8}{Q_3^2} \log^2\left(2\frac{Q_3}{Q_3}\right) \\ & + Q_3^2 \left[-\frac{130}{27Q_3^4} + \frac{76}{9Q_3^4} \log\left(2\frac{Q_3}{Q_3}\right) - \frac{40}{9Q_3^4} \log^2\left(2\frac{Q_3}{Q_3}\right) \right] \\ & + \delta \left[-\frac{18}{Q_3^3} + \frac{20}{Q_3^3} \log\left(2\frac{Q_3}{Q_3}\right) - \frac{8}{Q_3^3} \log^2\left(2\frac{Q_3}{Q_3}\right) \right] + \mathcal{O}\left(Q_3^4, \delta^2, \delta Q_3^2\right), \end{aligned} \quad (\text{B.15})$$

$$\begin{aligned} F_{123}(2) = & -6\zeta_3 + Q_3^2 \left[\frac{18}{Q_3^2} - \frac{12}{Q_3^2} \log\left(2\frac{Q_3}{Q_3}\right) \right], \\ & + \delta \left[-\frac{24}{Q_3} + \frac{24}{Q_3} \log\left(2\frac{Q_3}{Q_3}\right) - \frac{16}{Q_3} \log^2\left(2\frac{Q_3}{Q_3}\right) \right] + \mathcal{O}\left(Q_3^4, \delta^2, \delta Q_3^2\right). \end{aligned} \quad (\text{B.16})$$

In the corner regions one has to expand the $\mathcal{P}_i(z)$ for three different z , namely $z = 0, 1, \infty$. However, from the relations in (A.15) one can relate $\mathcal{P}_i(z)$ to $\mathcal{P}_i(1/z)$, so only $z = 0, 1$ are needed in practice.

⁵In the supplementary material file `cornerexpansions.txt`, we provide the full expansions needed for all corner regions.

The $\hat{\Pi}$ in region C_3 are given by

$$\begin{aligned} \frac{\hat{\Pi}_1}{c_s} &= \frac{1}{Q_3^2} \left[\frac{192}{Q_3^2} \right] + \frac{3568}{15Q_3^4} - \frac{2048}{5Q_3^4} \zeta_3 + \frac{3776}{9Q_3^4} \log \left(2 \frac{Q_3}{Q_3} \right) - \frac{256}{Q_3^4} \log^2 \left(2 \frac{Q_3}{Q_3} \right) \\ &+ Q_3^2 \left[\frac{39375808}{39375Q_3^6} - \frac{36864}{35Q_3^6} \zeta_3 + \frac{528896}{1125Q_3^6} \log \left(2 \frac{Q_3}{Q_3} \right) - \frac{12288}{25Q_3^6} \log^2 \left(2 \frac{Q_3}{Q_3} \right) \right] \\ &+ \frac{\delta^2}{Q_3^2} \left[\frac{1280}{9Q_3^4} - \frac{2560}{9Q_3^4} \log \left(2 \frac{Q_3}{Q_3} \right) \right] + \mathcal{O}(\delta^2, \delta^4 Q_3^{-2}), \end{aligned} \quad (\text{B.17})$$

$$\begin{aligned} \frac{\hat{\Pi}_4}{c_s} &= -\frac{12544}{45Q_3^4} + \frac{2048}{5Q_3^4} \zeta_3 + \frac{2048}{9Q_3^4} \log \left(2 \frac{Q_3}{Q_3} \right) \\ &+ Q_3^2 \left[-\frac{13533568}{13125Q_3^6} + \frac{49152}{35Q_3^6} \zeta_3 + \frac{1935872}{1125Q_3^6} \log \left(2 \frac{Q_3}{Q_3} \right) - \frac{14336}{25Q_3^6} \log^2 \left(2 \frac{Q_3}{Q_3} \right) \right] \\ &+ \mathcal{O}(\delta^2, Q_3^2, \delta^2 Q_3^2), \end{aligned} \quad (\text{B.18})$$

$$\begin{aligned} \frac{\hat{\Pi}_7}{c_s} &= -\frac{1024}{5Q_3^6} + \frac{8192}{5Q_3^6} \zeta_3 + \frac{8192}{9Q_3^6} \log \left(2 \frac{Q_3}{Q_3} \right) - \frac{\delta}{Q_3^2} \left[\frac{1024}{9Q_3^5} \right] \\ &+ \delta \left[-\frac{78295808}{13125Q_3^7} + \frac{196608}{35Q_3^7} \zeta_3 - \frac{17408}{1125Q_3^7} \log \left(2 \frac{Q_3}{Q_3} \right) + \frac{69632}{75Q_3^7} \log^2 \left(2 \frac{Q_3}{Q_3} \right) \right] \\ &+ Q_3^2 \left[-\frac{128872192}{39375Q_3^8} + \frac{98304}{35Q_3^8} \zeta_3 + \frac{13229056}{1125Q_3^8} \log \left(2 \frac{Q_3}{Q_3} \right) - \frac{323584}{75Q_3^8} \log^2 \left(2 \frac{Q_3}{Q_3} \right) \right] \\ &+ \mathcal{O}(\delta^2, \delta Q_3^2, \delta^3 Q_3^{-2}), \end{aligned} \quad (\text{B.19})$$

$$\begin{aligned} \frac{\hat{\Pi}_{17}}{c_s} &= \frac{1}{Q_3^2} \left[-\frac{512}{Q_3^4} + \frac{1024}{9Q_3^4} \log \left(2 \frac{Q_3}{Q_3} \right) \right] \\ &- \frac{112018624}{118125Q_3^6} + \frac{45056}{35Q_3^6} \zeta_3 - \frac{1769216}{1125Q_3^6} \log \left(2 \frac{Q_3}{Q_3} \right) + \frac{115712}{225Q_3^6} \log^2 \left(2 \frac{Q_3}{Q_3} \right) \\ &+ Q_3^2 \left[-\frac{139984302592}{24310125Q_3^8} + \frac{212992}{35Q_3^8} \zeta_3 - \frac{52059136}{25725Q_3^8} \log \left(2 \frac{Q_3}{Q_3} \right) + \frac{1101824}{735Q_3^8} \log^2 \left(2 \frac{Q_3}{Q_3} \right) \right] \\ &+ \frac{\delta^2}{Q_3^2} \left[-\frac{336896}{1125Q_3^6} + \frac{47104}{225Q_3^6} \log \left(2 \frac{Q_3}{Q_3} \right) \right] + \mathcal{O}(\delta^2, \delta^4 Q_3^{-2}), \end{aligned} \quad (\text{B.20})$$

$$\begin{aligned} \frac{\hat{\Pi}_{39}}{c_s} &= \frac{1}{Q_3^2} \left[-\frac{1024}{9Q_3^4} + \frac{1024}{9Q_3^4} \log \left(2 \frac{Q_3}{Q_3} \right) \right] \\ &- \frac{53725888}{118125Q_3^6} - \frac{4096}{35Q_3^6} \zeta_3 + \frac{725248}{1125Q_3^6} \log \left(2 \frac{Q_3}{Q_3} \right) - \frac{80896}{225Q_3^6} \log^2 \left(2 \frac{Q_3}{Q_3} \right) \\ &+ Q_3^2 \left[-\frac{75027492352}{121550625Q_3^8} - \frac{16384}{35Q_3^8} \zeta_3 - \frac{356996096}{385875Q_3^8} \log \left(2 \frac{Q_3}{Q_3} \right) - \frac{167936}{1225Q_3^8} \log^2 \left(2 \frac{Q_3}{Q_3} \right) \right] \\ &+ \frac{\delta^2}{Q_3^2} \left[\frac{11264}{1125Q_3^6} + \frac{47104}{225Q_3^6} \log \left(2 \frac{Q_3}{Q_3} \right) \right] + \mathcal{O}(\delta^2, \delta^4 Q_3^{-2}), \end{aligned} \quad (\text{B.21})$$

$$\begin{aligned} \frac{\hat{\Pi}_{54}}{c_s} &= \frac{\delta}{Q_3^2} \left[-\frac{1408}{9Q_3^5} - \frac{1024}{3Q_3^5} \log\left(2\frac{Q_3}{Q_3}\right) \right] \\ &+ \delta \left[-\frac{1937408}{1575Q_3^7} + \frac{24576}{35Q_3^7} \zeta_3 - \frac{687104}{225Q_3^7} \log\left(2\frac{Q_3}{Q_3}\right) + \frac{4096}{5Q_3^7} \log^2\left(2\frac{Q_3}{Q_3}\right) \right] \\ &+ \mathcal{O}(\delta Q_3^2, \delta^3 Q_3^{-2}, \delta^3), \end{aligned} \tag{B.22}$$

with the overall factor $c_s = \frac{2\pi\alpha_s(N_c^2-1)e_q^4}{(16\pi^2)^2}$. While all these expressions are finite when the small parameter δ tends to zero, some of them diverge when $Q_3^2 \rightarrow 0$. However, this divergence has no physical meaning, since that limit lies outside the region of validity of the OPE. The expansion of the $\hat{\Pi}$ in the other corner regions can be found in the supplementary material file `resultsgluon.txt`. Equivalent expressions are provided for the quark loop in `resultsquark.txt`.

B.2 Symmetric point

In this section, we write the expressions for the $\hat{\Pi}$ at the symmetric point $Q_1 = Q_2 = Q_3 = Q$.⁶ For the quark loop these are

$$\begin{aligned} \frac{16\pi^2 \hat{\Pi}_1^{\text{quark}}}{N_c e_q^4} &= -\frac{32}{3Q^4}, \\ \frac{16\pi^2 \hat{\Pi}_4^{\text{quark}}}{N_c e_q^4} &= \frac{2}{Q^4} \left(-\frac{352}{27} + \frac{128}{81} \Delta^{(1)} \right), \\ \frac{16\pi^2 \hat{\Pi}_7^{\text{quark}}}{N_c e_q^4} &= \frac{1}{Q^6} \left(-\frac{352}{27} + \frac{128}{81} \Delta^{(1)} \right), \\ \frac{16\pi^2 \hat{\Pi}_{17}^{\text{quark}}}{N_c e_q^4} &= \frac{1}{Q^6} \left(-\frac{384}{27} + \frac{192}{81} \Delta^{(1)} \right), \\ \frac{16\pi^2 \hat{\Pi}_{39}^{\text{quark}}}{N_c e_q^4} &= \frac{1}{Q^6} \left(\frac{320}{27} - \frac{64}{81} \Delta^{(1)} \right), \\ \frac{16\pi^2 \hat{\Pi}_{54}^{\text{quark}}}{N_c e_q^4} &= 0, \end{aligned} \tag{B.23}$$

where

$$\Delta^{(n)} \equiv \psi^{(n)}(1/3) - \psi^{(n)}(2/3). \tag{B.24}$$

and $\psi^{(n)}$ is the polygamma function of order n defined by

$$\psi^{(n)}(z) \equiv \frac{d^{n+1}}{dz^{n+1}} \log \Gamma(z). \tag{B.25}$$

One then has

$$\Delta^{(1)} \approx 7.031721716, \tag{B.26}$$

$$\Delta^{(3)} \approx 456.8524809. \tag{B.27}$$

⁶The associated $\hat{\Pi}$ are also available upon request.

These expressions agree with those given in ref. [36]. For the gluonic correction the result is

$$\begin{aligned}
 \frac{\hat{\Pi}_1^{\text{gluon}}}{c_s} &= \frac{1}{Q^4} \left(\frac{640\zeta_3}{3} + \frac{400}{9} \Delta^{(1)} - \frac{32}{27} \Delta^{(3)} \right), \\
 \frac{\hat{\Pi}_4^{\text{gluon}}}{c_s} &= \frac{1}{Q^4} \left(-32 + \frac{1664\zeta_3}{3} + \frac{1040}{9} \Delta^{(1)} - \frac{256}{81} \Delta^{(3)} \right), \\
 \frac{\hat{\Pi}_7^{\text{gluon}}}{c_s} &= \frac{1}{Q^6} \left(\frac{512\zeta_3}{3} + \frac{320}{9} \Delta^{(1)} - \frac{80}{81} \Delta^{(3)} \right), \\
 \frac{\hat{\Pi}_{17}^{\text{gluon}}}{c_s} &= \frac{1}{Q^6} \left(-32 + 384\zeta_3 + \frac{272}{3} \Delta^{(1)} - \frac{64}{27} \Delta^{(3)} \right), \\
 \frac{\hat{\Pi}_{39}^{\text{gluon}}}{c_s} &= \frac{1}{Q^6} \left(-\frac{32}{3} - 128\zeta_3 - \frac{272}{9} \Delta^{(1)} + \frac{64}{81} \Delta^{(3)} \right), \\
 \frac{\hat{\Pi}_{54}^{\text{gluon}}}{c_s} &= 0,
 \end{aligned} \tag{B.28}$$

where $c_s = \frac{2\pi\alpha_s(N_c^2-1)e_q^4}{(16\pi^2)^2}$.

Open Access. This article is distributed under the terms of the Creative Commons Attribution License ([CC-BY 4.0](https://creativecommons.org/licenses/by/4.0/)), which permits any use, distribution and reproduction in any medium, provided the original author(s) and source are credited.

References

- [1] T. Aoyama et al., *The anomalous magnetic moment of the muon in the Standard Model*, *Phys. Rept.* **887** (2020) 1 [[arXiv:2006.04822](https://arxiv.org/abs/2006.04822)] [[INSPIRE](#)].
- [2] MUON G-2 collaboration, *Muon ($g-2$) technical design report*, [arXiv:1501.06858](https://arxiv.org/abs/1501.06858) [[INSPIRE](#)].
- [3] M. Abe et al., *A new approach for measuring the muon anomalous magnetic moment and electric dipole moment*, *PTEP* **2019** (2019) 053C02 [[arXiv:1901.03047](https://arxiv.org/abs/1901.03047)] [[INSPIRE](#)].
- [4] MUON G-2 collaboration, *Final report of the muon E821 anomalous magnetic moment measurement at BNL*, *Phys. Rev. D* **73** (2006) 072003 [[hep-ex/0602035](https://arxiv.org/abs/hep-ex/0602035)] [[INSPIRE](#)].
- [5] T. Aoyama, M. Hayakawa, T. Kinoshita and M. Nio, *Complete tenth-order QED contribution to the muon $g-2$* , *Phys. Rev. Lett.* **109** (2012) 111808 [[arXiv:1205.5370](https://arxiv.org/abs/1205.5370)] [[INSPIRE](#)].
- [6] T. Aoyama, T. Kinoshita and M. Nio, *Theory of the anomalous magnetic moment of the electron*, *Atoms* **7** (2019) 28 [[INSPIRE](#)].
- [7] A. Czarnecki, W.J. Marciano and A. Vainshtein, *Refinements in electroweak contributions to the muon anomalous magnetic moment*, *Phys. Rev. D* **67** (2003) 073006 [*Erratum ibid.* **73** (2006) 119901] [[hep-ph/0212229](https://arxiv.org/abs/hep-ph/0212229)] [[INSPIRE](#)].
- [8] C. Gnendiger, D. Stöckinger and H. Stöckinger-Kim, *The electroweak contributions to $(g-2)_\mu$ after the Higgs boson mass measurement*, *Phys. Rev. D* **88** (2013) 053005 [[arXiv:1306.5546](https://arxiv.org/abs/1306.5546)] [[INSPIRE](#)].

- [9] M. Davier, A. Hoecker, B. Malaescu and Z. Zhang, *Reevaluation of the hadronic vacuum polarisation contributions to the Standard Model predictions of the muon $g - 2$ and $\alpha(m_Z^2)$ using newest hadronic cross-section data*, *Eur. Phys. J. C* **77** (2017) 827 [[arXiv:1706.09436](#)] [[INSPIRE](#)].
- [10] A. Keshavarzi, D. Nomura and T. Teubner, *Muon $g - 2$ and $\alpha(M_Z^2)$: a new data-based analysis*, *Phys. Rev. D* **97** (2018) 114025 [[arXiv:1802.02995](#)] [[INSPIRE](#)].
- [11] G. Colangelo, M. Hoferichter and P. Stoffer, *Two-pion contribution to hadronic vacuum polarization*, *JHEP* **02** (2019) 006 [[arXiv:1810.00007](#)] [[INSPIRE](#)].
- [12] M. Hoferichter, B.-L. Hoid and B. Kubis, *Three-pion contribution to hadronic vacuum polarization*, *JHEP* **08** (2019) 137 [[arXiv:1907.01556](#)] [[INSPIRE](#)].
- [13] M. Davier, A. Hoecker, B. Malaescu and Z. Zhang, *A new evaluation of the hadronic vacuum polarisation contributions to the muon anomalous magnetic moment and to $\alpha(m_Z^2)$* , *Eur. Phys. J. C* **80** (2020) 241 [*Erratum ibid.* **80** (2020) 410] [[arXiv:1908.00921](#)] [[INSPIRE](#)].
- [14] A. Keshavarzi, D. Nomura and T. Teubner, *$g - 2$ of charged leptons, $\alpha(M_Z^2)$, and the hyperfine splitting of muonium*, *Phys. Rev. D* **101** (2020) 014029 [[arXiv:1911.00367](#)] [[INSPIRE](#)].
- [15] A. Kurz, T. Liu, P. Marquard and M. Steinhauser, *Hadronic contribution to the muon anomalous magnetic moment to next-to-next-to-leading order*, *Phys. Lett. B* **734** (2014) 144 [[arXiv:1403.6400](#)] [[INSPIRE](#)].
- [16] G. Colangelo, M. Hoferichter, A. Nyffeler, M. Passera and P. Stoffer, *Remarks on higher-order hadronic corrections to the muon $g - 2$* , *Phys. Lett. B* **735** (2014) 90 [[arXiv:1403.7512](#)] [[INSPIRE](#)].
- [17] T. Blum et al., *Hadronic light-by-light scattering contribution to the muon anomalous magnetic moment from lattice QCD*, *Phys. Rev. Lett.* **124** (2020) 132002 [[arXiv:1911.08123](#)] [[INSPIRE](#)].
- [18] J. Bijnens, E. Pallante and J. Prades, *Hadronic light by light contributions to the muon $g - 2$ in the large N_c limit*, *Phys. Rev. Lett.* **75** (1995) 1447 [*Erratum ibid.* **75** (1995) 3781] [[hep-ph/9505251](#)] [[INSPIRE](#)].
- [19] J. Bijnens, E. Pallante and J. Prades, *Analysis of the hadronic light by light contributions to the muon $g - 2$* , *Nucl. Phys. B* **474** (1996) 379 [[hep-ph/9511388](#)] [[INSPIRE](#)].
- [20] M. Hayakawa and T. Kinoshita, *Pseudoscalar pole terms in the hadronic light by light scattering contribution to muon $g - 2$* , *Phys. Rev. D* **57** (1998) 465 [*Erratum ibid.* **66** (2002) 019902] [[hep-ph/9708227](#)] [[INSPIRE](#)].
- [21] J. Bijnens, E. Pallante and J. Prades, *Comment on the pion pole part of the light by light contribution to the muon $g - 2$* , *Nucl. Phys. B* **626** (2002) 410 [[hep-ph/0112255](#)] [[INSPIRE](#)].
- [22] M. Hayakawa and T. Kinoshita, *Comment on the sign of the pseudoscalar pole contribution to the muon $g - 2$* , [[hep-ph/0112102](#)] [[INSPIRE](#)].
- [23] J. Prades, E. de Rafael and A. Vainshtein, *The hadronic light-by-light scattering contribution to the muon and electron anomalous magnetic moments*, *Adv. Ser. Direct. High Energy Phys.* **20** (2009) 303 [[arXiv:0901.0306](#)] [[INSPIRE](#)].
- [24] G. Colangelo, M. Hoferichter, M. Procura and P. Stoffer, *Dispersion relation for hadronic light-by-light scattering: theoretical foundations*, *JHEP* **09** (2015) 074 [[arXiv:1506.01386](#)] [[INSPIRE](#)].

- [25] P. Masjuan and P. Sánchez-Puertas, *Pseudoscalar-pole contribution to the $(g_\mu - 2)$: a rational approach*, *Phys. Rev. D* **95** (2017) 054026 [[arXiv:1701.05829](#)] [[INSPIRE](#)].
- [26] M. Hoferichter, B.-L. Hoid, B. Kubis, S. Leupold and S.P. Schneider, *Dispersion relation for hadronic light-by-light scattering: pion pole*, *JHEP* **10** (2018) 141 [[arXiv:1808.04823](#)] [[INSPIRE](#)].
- [27] A. Gérardin, H.B. Meyer and A. Nyffeler, *Lattice calculation of the pion transition form factor with $N_f = 2 + 1$ Wilson quarks*, *Phys. Rev. D* **100** (2019) 034520 [[arXiv:1903.09471](#)] [[INSPIRE](#)].
- [28] G. Colangelo, M. Hoferichter, M. Procura and P. Stoffer, *Dispersion relation for hadronic light-by-light scattering: two-pion contributions*, *JHEP* **04** (2017) 161 [[arXiv:1702.07347](#)] [[INSPIRE](#)].
- [29] V. Pauk and M. Vanderhaeghen, *Single meson contributions to the muon's anomalous magnetic moment*, *Eur. Phys. J. C* **74** (2014) 3008 [[arXiv:1401.0832](#)] [[INSPIRE](#)].
- [30] I. Danilkin and M. Vanderhaeghen, *Light-by-light scattering sum rules in light of new data*, *Phys. Rev. D* **95** (2017) 014019 [[arXiv:1611.04646](#)] [[INSPIRE](#)].
- [31] F. Jegerlehner, *The anomalous magnetic moment of the muon*, Springer, Cham, Switzerland (2017) [[INSPIRE](#)].
- [32] M. Knecht, S. Narison, A. Rabemananjara and D. Rabetiarivony, *Scalar meson contributions to a_μ from hadronic light-by-light scattering*, *Phys. Lett. B* **787** (2018) 111 [[arXiv:1808.03848](#)] [[INSPIRE](#)].
- [33] G. Eichmann, C.S. Fischer and R. Williams, *Kaon-box contribution to the anomalous magnetic moment of the muon*, *Phys. Rev. D* **101** (2020) 054015 [[arXiv:1910.06795](#)] [[INSPIRE](#)].
- [34] P. Roig and P. Sanchez-Puertas, *Axial-vector exchange contribution to the hadronic light-by-light piece of the muon anomalous magnetic moment*, *Phys. Rev. D* **101** (2020) 074019 [[arXiv:1910.02881](#)] [[INSPIRE](#)].
- [35] J.H. Kühn, A.I. Onishchenko, A.A. Pivovarov and O.L. Veretin, *Heavy mass expansion, light by light scattering and the anomalous magnetic moment of the muon*, *Phys. Rev. D* **68** (2003) 033018 [[hep-ph/0301151](#)] [[INSPIRE](#)].
- [36] G. Colangelo, F. Hagelstein, M. Hoferichter, L. Laub and P. Stoffer, *Longitudinal short-distance constraints for the hadronic light-by-light contribution to $(g - 2)_\mu$ with large- N_c Regge models*, *JHEP* **03** (2020) 101 [[arXiv:1910.13432](#)] [[INSPIRE](#)].
- [37] G. Colangelo, F. Hagelstein, M. Hoferichter, L. Laub and P. Stoffer, *Short-distance constraints on hadronic light-by-light scattering in the anomalous magnetic moment of the muon*, *Phys. Rev. D* **101** (2020) 051501 [[arXiv:1910.11881](#)] [[INSPIRE](#)].
- [38] M. Knecht and A. Nyffeler, *Hadronic light by light corrections to the muon $g - 2$: the pion pole contribution*, *Phys. Rev. D* **65** (2002) 073034 [[hep-ph/0111058](#)] [[INSPIRE](#)].
- [39] T. Kinoshita, B. Nizic and Y. Okamoto, *Hadronic contributions to the anomalous magnetic moment of the muon*, *Phys. Rev. D* **31** (1985) 2108 [[INSPIRE](#)].
- [40] T. Goecke, C.S. Fischer and R. Williams, *Hadronic light-by-light scattering in the muon $g - 2$: a Dyson-Schwinger equation approach*, *Phys. Rev. D* **83** (2011) 094006 [[Erratum ibid.](#) **86** (2012) 099901] [[arXiv:1012.3886](#)] [[INSPIRE](#)].

- [41] R. Boughezal and K. Melnikov, *Hadronic light-by-light scattering contribution to the muon magnetic anomaly: constituent quark loops and QCD effects*, *Phys. Lett. B* **704** (2011) 193 [[arXiv:1104.4510](#)] [[INSPIRE](#)].
- [42] D. Greynat and E. de Rafael, *Hadronic contributions to the muon anomaly in the constituent chiral quark model*, *JHEP* **07** (2012) 020 [[arXiv:1204.3029](#)] [[INSPIRE](#)].
- [43] P. Masjuan and M. Vanderhaeghen, *Ballpark prediction for the hadronic light-by-light contribution to the muon $(g - 2)_\mu$* , *J. Phys. G* **42** (2015) 125004 [[arXiv:1212.0357](#)] [[INSPIRE](#)].
- [44] A.E. Dorokhov, A.E. Radzhabov and A.S. Zhevlakov, *Dynamical quark loop light-by-light contribution to muon $g - 2$ within the nonlocal chiral quark model*, *Eur. Phys. J. C* **75** (2015) 417 [[arXiv:1502.04487](#)] [[INSPIRE](#)].
- [45] K. Melnikov and A. Vainshtein, *Hadronic light-by-light scattering contribution to the muon anomalous magnetic moment revisited*, *Phys. Rev. D* **70** (2004) 113006 [[hep-ph/0312226](#)] [[INSPIRE](#)].
- [46] K. Melnikov and A. Vainshtein, *On dispersion relations and hadronic light-by-light scattering contribution to the muon anomalous magnetic moment*, [arXiv:1911.05874](#) [[INSPIRE](#)].
- [47] J. Leutgeb and A. Rebhan, *Axial vector transition form factors in holographic QCD and their contribution to the anomalous magnetic moment of the muon*, *Phys. Rev. D* **101** (2020) 114015 [[arXiv:1912.01596](#)] [[INSPIRE](#)].
- [48] L. Cappiello, O. Catà, G. D'Ambrosio, D. Greynat and A. Iyer, *Axial-vector and pseudoscalar mesons in the hadronic light-by-light contribution to the muon $(g - 2)$* , *Phys. Rev. D* **102** (2020) 016009 [[arXiv:1912.02779](#)] [[INSPIRE](#)].
- [49] M. Knecht, *On some short-distance properties of the fourth-rank hadronic vacuum polarization tensor and the anomalous magnetic moment of the muon*, *JHEP* **08** (2020) 056 [[arXiv:2005.09929](#)] [[INSPIRE](#)].
- [50] P. Masjuan, P. Roig and P. Sanchez-Puertas, *The interplay of transverse degrees of freedom and axial-vector mesons with short-distance constraints in $g - 2$* , [arXiv:2005.11761](#) [[INSPIRE](#)].
- [51] J. Lüdtkke and M. Procura, *Effects of longitudinal short-distance constraints on the hadronic light-by-light contribution to the muon $g - 2$* , *Eur. Phys. J. C* **80** (2020) 1108 [[arXiv:2006.00007](#)] [[INSPIRE](#)].
- [52] M. Hoferichter and P. Stoffer, *Asymptotic behavior of meson transition form factors*, *JHEP* **05** (2020) 159 [[arXiv:2004.06127](#)] [[INSPIRE](#)].
- [53] M.A. Shifman, A.I. Vainshtein and V.I. Zakharov, *QCD and resonance physics. Theoretical foundations*, *Nucl. Phys. B* **147** (1979) 385 [[INSPIRE](#)].
- [54] J. Bijnens, N. Hermansson-Truedsson and A. Rodríguez-Sánchez, *Short-distance constraints for the HLbL contribution to the muon anomalous magnetic moment*, *Phys. Lett. B* **798** (2019) 134994 [[arXiv:1908.03331](#)] [[INSPIRE](#)].
- [55] I.I. Balitsky and A.V. Yung, *Proton and neutron magnetic moments from QCD sum rules*, *Phys. Lett. B* **129** (1983) 328 [[INSPIRE](#)].
- [56] B.L. Ioffe and A.V. Smilga, *Nucleon magnetic moments and magnetic properties of vacuum in QCD*, *Nucl. Phys. B* **232** (1984) 109 [[INSPIRE](#)].

- [57] J. Bijnens, N. Hermansson-Truedsson, L. Laub and A. Rodríguez-Sánchez, *Short-distance HLbL contributions to the muon anomalous magnetic moment beyond perturbation theory*, *JHEP* **10** (2020) 203 [[arXiv:2008.13487](#)] [[INSPIRE](#)].
- [58] J. Aldins, T. Kinoshita, S.J. Brodsky and A.J. Dufner, *Photon-photon scattering contribution to the sixth order magnetic moments of the muon and electron*, *Phys. Rev. D* **1** (1970) 2378 [[INSPIRE](#)].
- [59] J.A.M. Vermaseren, *New features of FORM*, [math-ph/0010025](#) [[INSPIRE](#)].
- [60] P. Maierhöfer, J. Usovitsch and P. Uwer, *Kira — a Feynman integral reduction program*, *Comput. Phys. Commun.* **230** (2018) 99 [[arXiv:1705.05610](#)] [[INSPIRE](#)].
- [61] T.G. Birtwright, E.W.N. Glover and P. Marquard, *Master integrals for massless two-loop vertex diagrams with three offshell legs*, *JHEP* **09** (2004) 042 [[hep-ph/0407343](#)] [[INSPIRE](#)].
- [62] F. Chavez and C. Duhr, *Three-mass triangle integrals and single-valued polylogarithms*, *JHEP* **11** (2012) 114 [[arXiv:1209.2722](#)] [[INSPIRE](#)].
- [63] J. Kodaira, S. Matsuda, T. Muta, K. Sasaki and T. Uematsu, *QCD effects in polarized electroproduction*, *Phys. Rev. D* **20** (1979) 627 [[INSPIRE](#)].
- [64] J. Kodaira, S. Matsuda, K. Sasaki and T. Uematsu, *QCD higher order effects in spin dependent deep inelastic electroproduction*, *Nucl. Phys. B* **159** (1979) 99 [[INSPIRE](#)].
- [65] J. Kodaira, *QCD higher order effects in polarized electroproduction: flavor singlet coefficient functions*, *Nucl. Phys. B* **165** (1980) 129 [[INSPIRE](#)].
- [66] FLAVOUR LATTICE AVERAGING GROUP collaboration, *FLAG review 2019: Flavour Lattice Averaging Group (FLAG)*, *Eur. Phys. J. C* **80** (2020) 113 [[arXiv:1902.08191](#)] [[INSPIRE](#)].
- [67] F. Herren and M. Steinhauser, *Version 3 of RunDec and CRunDec*, *Comput. Phys. Commun.* **224** (2018) 333 [[arXiv:1703.03751](#)] [[INSPIRE](#)].
- [68] N.I. Usyukina and A.I. Davydychev, *New results for two loop off-shell three point diagrams*, *Phys. Lett. B* **332** (1994) 159 [[hep-ph/9402223](#)] [[INSPIRE](#)].